

AN ABSTRACT OF THE THESIS OF

Stephen L. Weitz for the degree of Doctor of Philosophy
in Biochemistry and Biophysics presented on June 6, 1984.

Title: Alternatives to the DNA Precursor-Synthesizing
Enzyme Complex Hypothesis

Abstract approved:

Redacted for privacy

Christopher K. Mathews

Investigators have been studying an aggregate containing enzymes of deoxyribonucleoside triphosphate biosynthesis in T4-phage infected bacteria. They suggest that it behaves as an organized complex, efficiently channeling DNA precursors to the replication apparatus. Previous work has suggested that about 10 enzyme activities remain associated through several fractionation steps. This multi-enzyme aggregate has been reported to sediment through sucrose gradients at 15-20 S. Also, individual activities are kinetically coupled in crude preparations of this aggregate, such that in vitro it can initiate catalysis of multistep pathways with virtually no lag and with low accumulation of intermediates.

However, work presented here shows that aggregation of thymidylate synthase, the key enzyme of all kinetic coupling studies, is not observed when either of its two

enzyme cofactors is present. Evidence suggests that the enzyme binds to ribosomal subunits due to an affinity for single-stranded nucleic acids under conditions of low ionic strength. This unexpected affinity, present even in the absence of other T4 proteins, can be explained as a consequence of the enzyme being part of the morphological structure of the virus particle.

Nucleoside diphosphate kinase and adenylate kinase, two host enzymes of the proposed complex, are shown to sediment with the exact same pattern in uninfected or infected cells. Thus, aggregation of these dNTP-synthesizing enzymes is not influenced qualitatively or quantitatively by the increased number of DNA replication forks present in an infected cell. Contrary to previous reports, sedimentation values in sucrose gradients are 30-50 S irrespective of the number of enzyme activities present in the aggregate. This aggregation is sensitive to physiological concentrations of salt. Evidence suggests that aggregation is due to low-salt induced binding of proteins to ribosomal subunits.

In situ evidence of DNA-precursor channeling in sucrose plasmolyzed, T4 infected cells is shown not to be consistent with results obtained with other plasmolysis or gentle lysate systems. The discrepancy can be resolved by the demonstration that sucrose plasmolyzed, T4 infected, cells may have relatively intact membranes.

Alternatives to the DNA Precursor-Synthesizing
Enzyme Complex Hypothesis

by

Stephen L. Weitz

A thesis

Submitted to

Oregon State University

in partial fulfillment of
the requirements for the
degree of

Doctor of Philosophy

Completed June 6, 1984

Commencement June 1985

APPROVED:

Redacted for privacy

Professor of Biochemistry and Biophysics in charge of major

Redacted for privacy

Head of department of Biochemistry and Biophysics

Redacted for privacy

Dean of Graduate School

Date thesis is presented: June 6, 1984

Typed by Stephen L. Weitz

This work is dedicated to NATURE
in all its glorious manifestations
and to the SOURCE
from which it springs

Acknowledgements

I wish to thank Dr. Christopher K. Mathews for the opportunity to do research in his laboratory. His creativity, vitality, and dedication to the field of Biochemistry has served as a source of inspiration.

My earliest interest in Biochemistry was kindled by Frederick Fisher. His encouragement and stimulating teaching greatly influenced me.

Many thanks go out to the faculty members who have taken time from their busy schedules to take part in helpful discussions and committee meetings. They include Dr. Ken Van Holde, Dr. Mike Schimerlik, Dr. Sonia Anderson, Dr. Stephen Kaattari, and Dr. Anglemier.

I owe a special thanks to each of the members in this laboratory: to Gerry Lasser for his patient technical advice and skillful assistance; to Joe Booth, Geoff Sargent, and Janet Leeds for many useful and enjoyable bull sessions; to Mary Slabaugh for added perspective; to Craig Spiro for his ever present dry and witty humor.

Finally, I would like to thank Susan, my wife, and our parents for their patience and encouragement.

TABLE OF CONTENTS

CHAPTER	PAGE
I. INTRODUCTION	1
Control and Fidelity of DNA Replication	1
T4 DNA Precursor Biosynthesis	2
Multienzyme Complexes and Precursor Compartmentation	8
Present Work	15
II. MATERIALS AND METHODS	17
Phage, Bacteria, and Culture Conditions	17
Isoelectric Focusing	18
Purification of Thymidylate Synthase	19
Purification of dCMP Hydroxymethylase	19
Sucrose Gradient Centrifugation	20
Nucleic Acids	21
C Labeling of Early Phage Enzymes	21
Binding Purified Proteins to Affi-gel Matrix	22
5' Nucleotidase Assays	22
Computer Simulations of Coupled Activity	23
<u>In Situ</u> Labeled Nucleotide Incorporation	24
Abbreviations Used	25
III RESULTS	27
PART 1: T4 Thymidylate Synthase Binds Nucleic Acid	27
Isoelectric focusing of multienzyme aggregate	27
Kinetic coupling in aggregated T4 thymidylate synthase	29
Effect of Mg ⁺⁺ and its reversibility	31
Sensitivity of aggregation to monovalent cations, Effect of substrates on sedimentation profiles	32
Aggregation of T4 thymidylate synthase in the absence of other phage proteins	35
Association of purified T4 thymidylate synthase with nucleic acid	38
PART 2: Conditions for Aggregation of Other dNTP Synthesizing Enzymes	46
Cation sensitivity of rapidly sedimenting protein Host enzyme aggregation studied with uninfected cells	46
Non-association of purified T4 dCMP hydroxy- methylase with rRNA	49

Assay for protein-protein interaction using an enzyme-bound column	51
PART 3: Observations Regarding Kinetically Coupled Activity	61
Effect of Mg ⁺⁺ ion on kinetically coupled assay	61
Existence of additional pathways	62
Non-reproducibility of initial result	66
Consensus value computer simulation	66
PART 4: Compartmentation of Nucleotides <u>In Situ</u> in plasmolysed cells	72
Verification of 5' nucleotidase activity in T4 infected <u>E. coli</u>	72
Membrane vs enzyme compartmentation	74
Lack of correlation with other permeablization methods	76
IV. DISCUSSION	79
PART 1: Enzyme Aggregation and Sedimentation	79
T4 thymidylate synthase binds single stranded nucleic acid	79
Nature of protein-protein interactions	82
Behavior of polyelectrolyte molecules	85
Nonspecific ionic interactions as suggested cause of enzyme aggregation	86
PART 2: Concluding Summary	90
V. BIBLIOGRAPHY	93

LIST OF FIGURES

<u>Figure</u>		<u>Page</u>
1	Reactions of DNA precursor biosynthesis in T4 phage-infected <u>E. coli</u> .	3
2	Map positions of T4 genes coding for enzymes of DNA precursor biosynthesis.	5
3	Schematic diagram of baseplate hexagon and star forms.	9
4	Structure of dihydropteroyl hexaglutamate and possible interactions with baseplate wedge and hub components.	10
5	Speculative view of the T4 dNTP-synthesizing complex.	11
6	Sedimentation analysis of enzyme activities in a crude extract of T4-infected <u>E. coli B</u> .	13
7	Deoxynucleotide incorporation <u>in situ</u> at different concentrations.	14
8	Production of dTTP by aggregated enzymes.	16
9	Isoelectric focusing of activities in an of phage-infected <u>E. coli</u> 201.	28
10	Sedimentation profile of activities in a 30-50% ammonium sulfate precipitate from a crude extract of T4-infected <u>E. coli</u> .	30
11	Effect of Mg ⁺⁺ upon sedimentation of T4 thymidylate synthase.	33
12	Effect of K ⁺ upon sedimentation of T4 thymidylate synthase.	34
13	Effect of substrates upon sedimentation of T4 thymidylate synthase.	36
14	Sedimentation profile of a mixture of FdUMP + CH FH + thymidylate synthase + rRNA.	37
15	Sedimentation profile of T4 thymidylate synthase expressed from the <u>td</u> gene cloned into a high-expression plasmid vector.	39
16	Binding of T4 thymidylate synthase to single-stranded DNA.	41

17	Lack of binding of thymidylate synthase to double-stranded DNA.	42
18	Binding of T4 thymidylate synthase to purified <u>E. coli</u> rRNA.	43
19	Binding of T4 thymidylate synthase to nucleic acid homopolymers.	45
20	Effect of Mg ⁺⁺ upon sedimentation of protein as estimated by A(280-310).	47
21	Individual enzyme profiles with and without 10 mM Mg ⁺⁺ .	48
22	Enzyme activity profile of host adenylate kinase and nucleoside diphosphate kinase from sucrose gradient sedimentation of <u>uninfected E. coli</u> extract.	50
23	Polyacrylamide gel electrophoresis of purified phage dCMP hydroxymethylase and <u>E. coli</u> nucleoside diphosphate kinase.	52
24	Lack of binding of T4 dCMP hydroxymethylase to purified <u>E. coli</u> rRNA.	53
25	Elution profile from an ethanolamine coupled Affi-Gel control column.	55
26	Elution profile from a bovine serum albumin coupled Affi-Gel control column.	56
27	Elution profile from an <u>E. coli</u> nucleoside diphosphate kinase bound Affi-Gel column	57
28	Elution profile from a T4 phage dihydrofolate reductase coupled Affi-Gel column.	58
29	Elution profile from a phage dCMP hydroxymethylase coupled Affi-Gel column.	59
30	Proposed pathways for <u>in vitro</u> kinetically coupled enzyme assay	63
31	5' nucleotidase assay of the top, middle, and bottom fractions of a sucrose gradient separation of an extract of T4-infected <u>E. coli</u> .	65
32	Program used to generate concentrations of nucleotides as a function of time for the	

	coupled assay shown in Figure 29A.	69
33	This reproduction of Figure 8 has been modified to include dTTP and dTDP concentrations from table 4A.	71
34	Assay of 5' nucleotidase activity in a crude extract of T4 infected <u>E. coli</u> .	73
35	DNA synthesis in plasmolysed and non plasmolysed wild-type T4-infected cells.	75
36	Effect of plasmolysis upon T4D-directed DNA synthesis <u>in situ</u> .	77
37	Inhibition of various thymidylate synthases by pteroylpolyglutamate as a function of the number of glutamate residues.	81
38	Diagram showing major chemical constituents of three fluid compartments.	87

LIST OF TABLES

<u>Table</u>		<u>Page</u>
1	Enzymes in T4 DNA precursor synthesis.	6
2	List of abbreviations.	26
3	Enzyme activities from rapidly sedimenting fraction of 5-20% sucrose gradients.	67
4	The tables present the various nucleotide concentrations at one minute intervals.	70
5	Forces that stabilize protein-protein subunit interactions.	84

Alternatives to the DNA Precursor-Synthesizing Enzyme Complex Hypothesis

I. INTRODUCTION

CONTROL AND FIDELITY OF DNA REPLICATION

Since the establishment of DNA as the self-replicating storehouse of genetic information in cells investigators have explored parameters that control the initiation and fidelity of replication; there is a consensus that control occurs through more than one mechanism. At least two levels of control exist for initiation of replication. All cells require communication between the system required for initiation and completion of DNA synthesis with those that monitor cellular size and nutritional state. Additionally, contact inhibition is vital for the orderly maintenance of morphological structure in multicellular organisms. Drug-induced gene amplification provides evidence for an additional level of control.

Many mechanisms have been demonstrated to control the fidelity of replication. The mutator/antimutator phenotype of any particular DNA replicase can provide variation in the fidelity of replication for a population of cells. The activity and specificity of particular repair enzymes can affect a cell's potential for coping with mutagenic

events. Finally, the maintenance of roughly equal concentrations of the four deoxyribonucleotide triphosphates at the site of replication is necessary for reducing the chances of base misincorporation during the process of DNA replication. This last parameter has been the object of investigation in this laboratory for many years. Bacteriophage T4 has been a system of choice for reasons that are discussed below.

T4 DNA PRECURSOR BIOSYNTHESIS

The enzyme pathways of T4 DNA precursor biosynthesis have been a completed story for more than a decade. Most of this information has been reviewed (Cohen, 1968; Mathews, 1971; Mathews, 1977). The pathways of DNA precursor biosynthesis in T4 infection are shown in Fig. 1. The major qualitative change upon infection is the production of hm-dCTP (see Table 2 for abbreviations) instead of dCTP, which accounts for the substitution in T-even phage DNA of HMC for cytosine. A further modification, the glucosylation of the hydroxymethyl groups in HMC, occurs after dNTP's have been polymerized into DNA (Erikson and Szybalski, 1964). Quantitatively, the rate of DNA synthesis increases up to tenfold relative to that seen in uninfected Escherichia coli . This increased rate of synthesis is accomplished by augmenting the cellular enzymes with virally induced

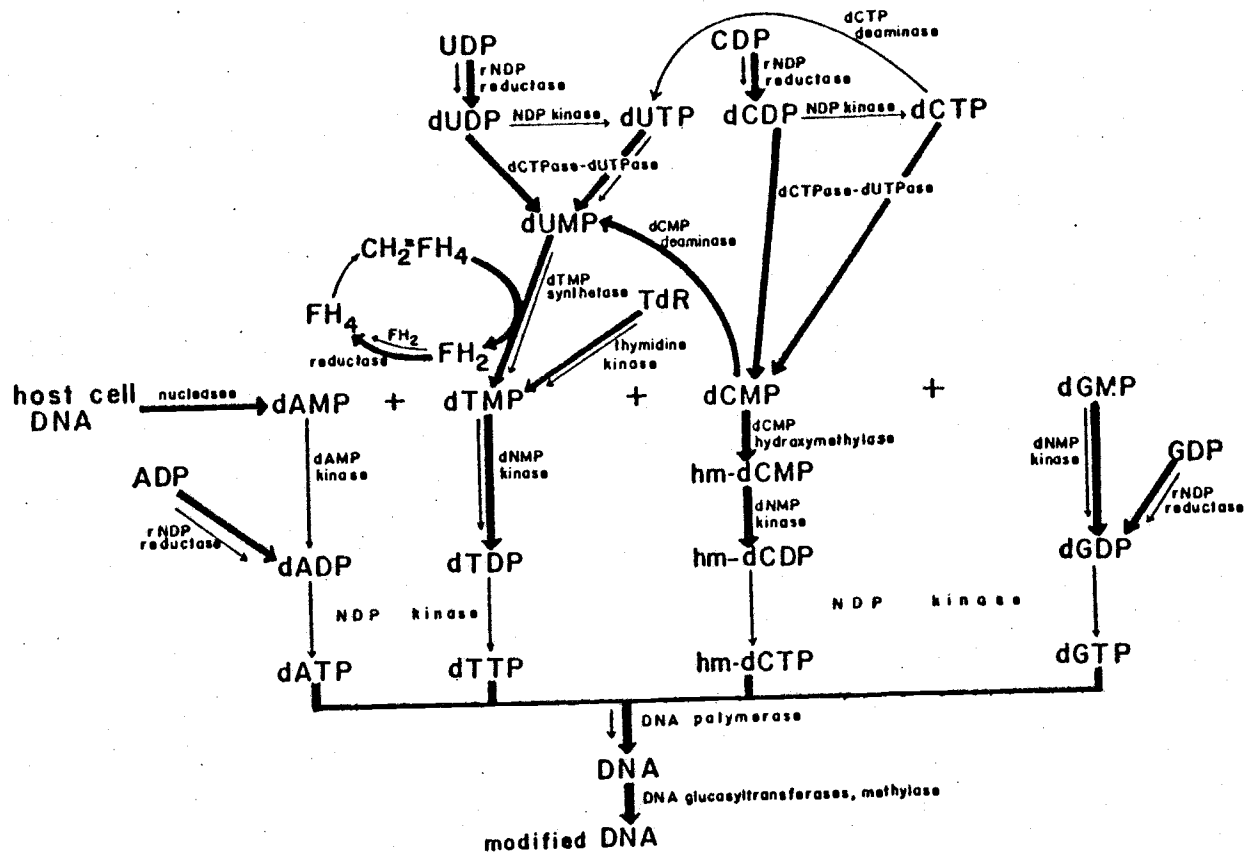


Figure 1. Reactions of DNA precursor biosynthesis in T4 phage-infected *E. coli*. Reactions catalyzed by virus-coded enzymes are identified with heavy arrows, and those catalyzed by preexisting host cell enzymes are denoted with light arrows. From *Bacteriophage T4* (1983) American Society for Microbiology.

enzymes which duplicate and enhance the preexisting dNTP synthetic activities. In addition to de novo nucleotide synthesis a substantial source of DNA precursors is the bacterial chromosome, whose breakdown can yield enough dNTP's to produce about 20 equivalents of phage DNA. Properties of the nucleases and other proteins involved in degradation of the host chromosome have been reviewed (Warner and Snustad, 1983).

The structural genes for all known T4 proteins involved in the synthesis of deoxyribonucleotides have been mapped. Figure 2 diagrams these map positions. The genes are scattered throughout most of the genome with the exception of the region between 80 and 120 kilobases, which codes for most of the structural proteins of the phage particle. All of the genes coding for enzymes of dNTP biosynthesis are expressed before the onset of DNA replication.

Some of the physical and catalytic properties of each of the enzymes of T4 deoxyribonucleotide metabolism are summarized in Table 1. Included here are the glucosyltransferases which alter HMC residues in newly synthesized DNA, even though they are not enzymes of DNA precursor metabolism per se. Three of the enzymes listed have counterparts in cells which are subject to complex feedback regulation. Of these only dCMP deaminase displays a regulatory pattern similar to that of its cellular homolog. Both it and the cellular dCTP deaminase display

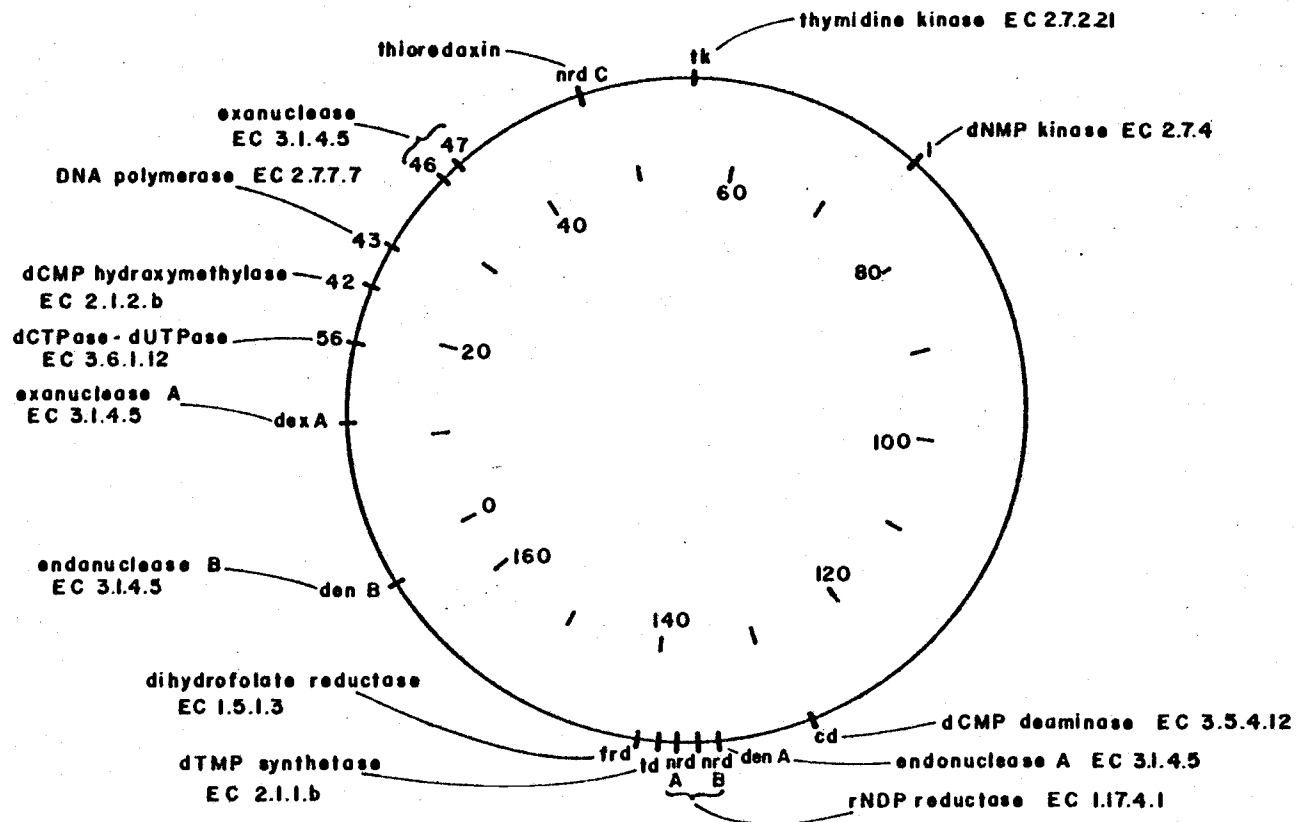


Figure 2. Map positions of T4 genes coding for enzymes of DNA precursor biosynthesis. The numbers in the interior represent distance in kilobases from the rIIA/rIIB cistron divide. From Bacteriophage T4 (1983) American society for Microbiology, Washington D.C.

TABLE I. Enzymes in T4 DNA precursor synthesis*

Enzyme	Reaction(s) catalyzed	Structural gene	Mutants available	Mol wt ($\times 10^3$)	
				Native	Subunit
dCMP hydroxymethylase	$dCMP \xrightarrow{CH_2FH_4} hm\text{-}dCMP$ FH_4	42	Amber, <i>ts</i>	60	27, 25 ^b
dTMP synthetase	$dUMP \xrightarrow{CH_2FH_4} dTMP$ FH_4	<i>td</i>	Nonlethal amber, missense, deletions	58	29
Dihydrofolate reductase	$FH_2 \xrightarrow{NADPH + H^+} FH_4$ $NADP^+$	<i>fd</i>	Nonlethal amber, deletions, missense	44.5 ^c	23 ^c
dNMP kinase	$dTMP \xrightarrow{ATP} dTDP$ $dUMP \xrightarrow{ATP} dUDP$ $hm\text{-}dCMP \xrightarrow{ATP} hm\text{-}dCDP$ ADP	1	Amber, <i>ts</i>	Unknown	22
(d)AMP kinase	$dAMP \xrightarrow{ATP} dADP$ ADP	Host gene		Unknown	Unknown
NDP kinase	$dNDP \xrightarrow{NTP} dNTP$ NDP	Host gene	One <i>cs</i> in <i>Salmonella</i>	110 ^d	15.5 ^d
dCTPase-dUTPase	$dCTP \xrightarrow{H_2O} dUMP$ $dUTP \xrightarrow{H_2O} dUMP$ PP_i $dCDP \xrightarrow{H_2O} dUDP$ P_i	56	Amber, <i>ts</i>	59	15
dCMP deaminase	$dCMP \xrightarrow{H_2O} dUMP$ NH_3	<i>cd</i>	Nonlethal missense	124, 129 ^e	20.2
Thymidine kinase	$TdR \xrightarrow{ATP} dTMP$ ADP	<i>tk</i>	Nonlethal missense; BUdR resistant	86	28
rNDP reductase	$CDP \xrightarrow{reduced\ thiorredoxin} dCDP$ $UDP \xrightarrow{reduced\ thiorredoxin} dUDP$ $GDP \xrightarrow{reduced\ thiorredoxin} dGDP$ $ADP \xrightarrow{reduced\ thiorredoxin} dADP$ $oxidized\ thiorredoxin$	<i>nrdA</i> , <i>nrdB</i>	Nonlethal missense, amber, deletions, folate analog resistant ^f	225	85 (<i>nrdA</i>), 35 (<i>nrdB</i>)
Thioredoxin	see above	<i>nrdC</i>	Nonlethal missense	10.4	10.4
DNA α -glucosyltransferase	$DNA\text{-}HMC \xrightarrow{UDP\text{-}glucose} \alpha\text{-glucosyl}\text{-}DNA\text{-}HMC$ UDP	<i>\alpha\text{-gt}</i>	Amber, missense (lethal in combination with β -gt)	Unknown	Unknown
DNA β -glucosyltransferase	$DNA\text{-}HMC \xrightarrow{UDP\text{-}glucose} \beta\text{-glucosyl}\text{-}DNA\text{-}HMC$ UDP	β -gt	Amber, missense (lethal in combination with α -gt)	Unknown	46 ^g

* Except as otherwise indicated, data are from sources cited in Mathews (1977).

^b North and Mathews (1977); O'Farrell, et al. (1973).

^c Pirobit et al. (1981).

^d Roisin and Kepes (1978).

^e G. W. Lasser, unpublished data.

^f Malev et al. (1972); Scoocca et al. (1969).

^g Johnson et al. (1976).

^h Huang and Buchanan (1974).

inhibition by dTTP and a nearly absolute requirement for dCTP for activity (Maley and Maley, 1982; Maley et al , 1967; Scocca et al , 1969). Unlike cellular ribonucleotide reductases the four activities of the T4 enzyme are not inhibited to any great degree by the negative allosteric effector dATP (Berglund, 1972). This is in accord with the need to produce as much phage DNA as is possible for packaging during phage assembly over the course of the lytic infection. Finally, T4 thymidine kinase, unlike its cellular counterpart, does not need the positive allosteric effector dCTP (Iwatsuki, 1977).

The synthesis of T4 DNA precursors is really an interplay between phage-encoded and host enzymes. Nucleoside diphosphokinase phosphorylates dNDP's to the corresponding dNTP's with a great lack of specificity in this final step of dNTP synthesis. The bacterial AMP-dAMP kinase is a non-essential enzyme because ribonucleotides enter the deoxyribonucleotide pool at the diphosphate level. However, the enzyme probably has survival value because it allows the phage to utilize dAMP generated from the breakdown of host DNA.

In addition to being part of the dNTP-synthesizing system two enzymes, thymidylate synthase and dihydrofolate reductase, have structural roles as components of the baseplate of the phage tail. It is beyond the scope of this work to review all of the evidence for such a dual role. The subject has been treated in detail by Kozloff

(1983) and Mathews and Allen (1983). The current theory suggests that the central hub and radial arms of the baseplate, Fig. 3, are stabilized by a dihydropteroylhexaglutamate bridge that spans between thymidylate synthase in the hub to dihydrofolate reductase found in each radial arm of the baseplate, Fig. 4. Kikuchi and King (1975) demonstrated that in the absence of central hub structures, 1/6th arms can assemble slowly into baseplate-like structures which are missing the central hub. Therefore, the proposed polyhexaglutamate bridge is needed only to increase the rate of assembly and add additional strength to a partially stabilized structure. The physical characteristics of thymidylate synthase as a structural protein will take on added significance when the sedimentation behavior of this enzyme is discussed later.

MULTIENZYME COMPLEXES AND PRECURSOR COMPARTMENTATION

For a number of years now this laboratory and that of Dr. G. R. Greenberg have been studying the possibility that DNA precursors are synthesized by a multienzyme complex, Fig. 5, which is physically and functionally linked to the T4 replication apparatus presently being characterized by Alberts and Nossal (1983). The T-even bacteriophage is an advantageous experimental system for several reasons. Most of the steps involved in DNA precursor synthesis and virtually all of DNA replication

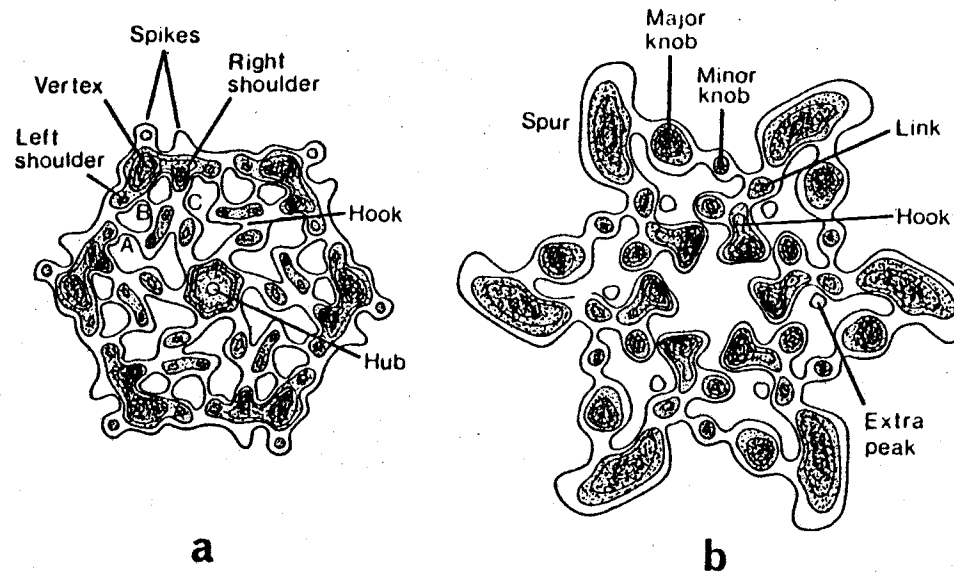


Figure 3. Schematic diagram of baseplate hexagon and star forms. The transformation from hexagon to star form is complex and involves rearrangement of most of the mass of the baseplate. It is not known whether the parts of the hub move to the outer radius or whether some proteins are actually lost. The star drawing does not include the thin fibrils often seen projecting from the vertices of stars derived from complete baseplates. These fibrils may be the gene 12 protein, which is folded up beneath the baseplate in the hexagonal state. From Bacteriophage T4 (1983) American Society for Microbiology, Wash. D.C.

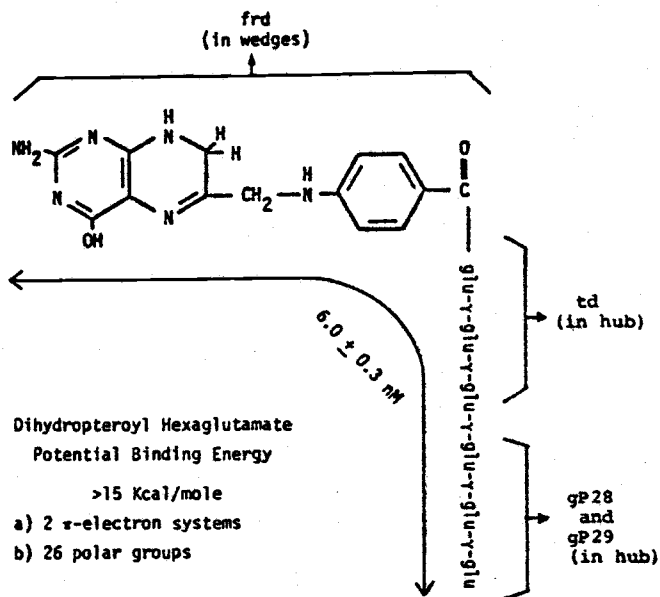


Figure 4. Structure of dihydropteroyl hexaglutamate and possible interactions with baseplate wedge and hub components, frd, Dihydrofolate reductase; td, Thymidylate synthase, From Bacteriophage T4 (1983) A.S.M.

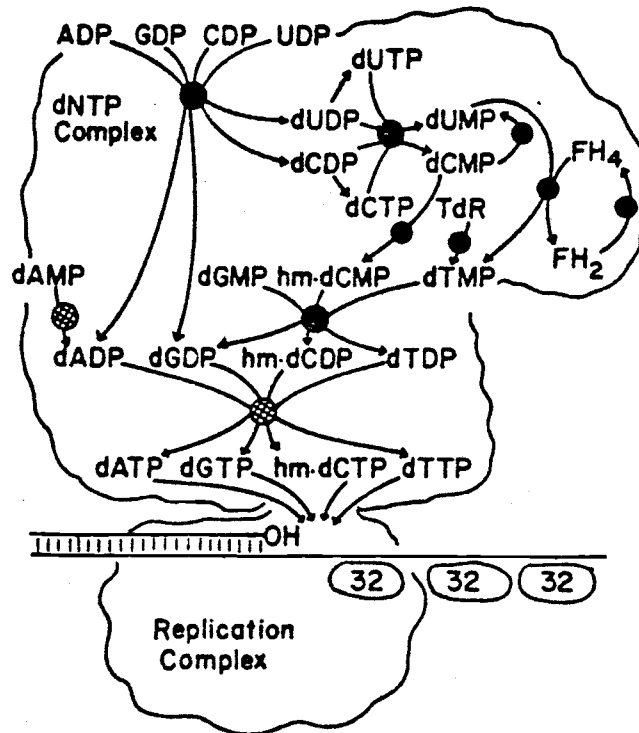


Figure 5. Speculative view of the T4 dNTP-synthesizing complex. Closed circles denote phage-coded enzymes; cross-hatched circles denote *E. coli* enzymes. From Bacteriophage T4 (1983) A.S.M., Wash. D.C.

are catalyzed by phage-coded enzymes. Upon infection the nucleic acid and protein metabolism in Escherichia coli is abruptly and completely redirected toward growth and reproduction of the phage. A large catalogue of mutants defective in viral functions is available. More recently, a number of phage genes have been cloned into high expression vectors, allowing investigators to study the properties of phage-coded enzymes in vitro and also in vivo in uninfected cells.

A great deal of data has been collected and interpreted to support the idea that T4 produces a dNTP-synthesizing enzyme complex which is juxtaposed in the cell with the T4 DNA polymerization apparatus. These interpretations state that the complex maintains local concentration gradients of DNA precursors at replication sites and hence contributes toward maintaining high rates of replication. Data for such assertions fall into three main conceptual categories. The first is protein-protein interactions between enzymes involved with dNTP synthesis and DNA polymerization, as manifested by enzyme rapid sedimentation in sucrose gradients in vitro (Reddy et al 1977), Fig. 6, and genetic mutant analysis in vivo (North et al 1976). The second consists of preferential incorporation of dNMP's over dNTP's into DNA in situ in sucrose plasmolysed cells, suggesting that distal DNA precursors have preferential access over the more immediate precursors to DNA polymerase, Fig. 7 (Reddy and

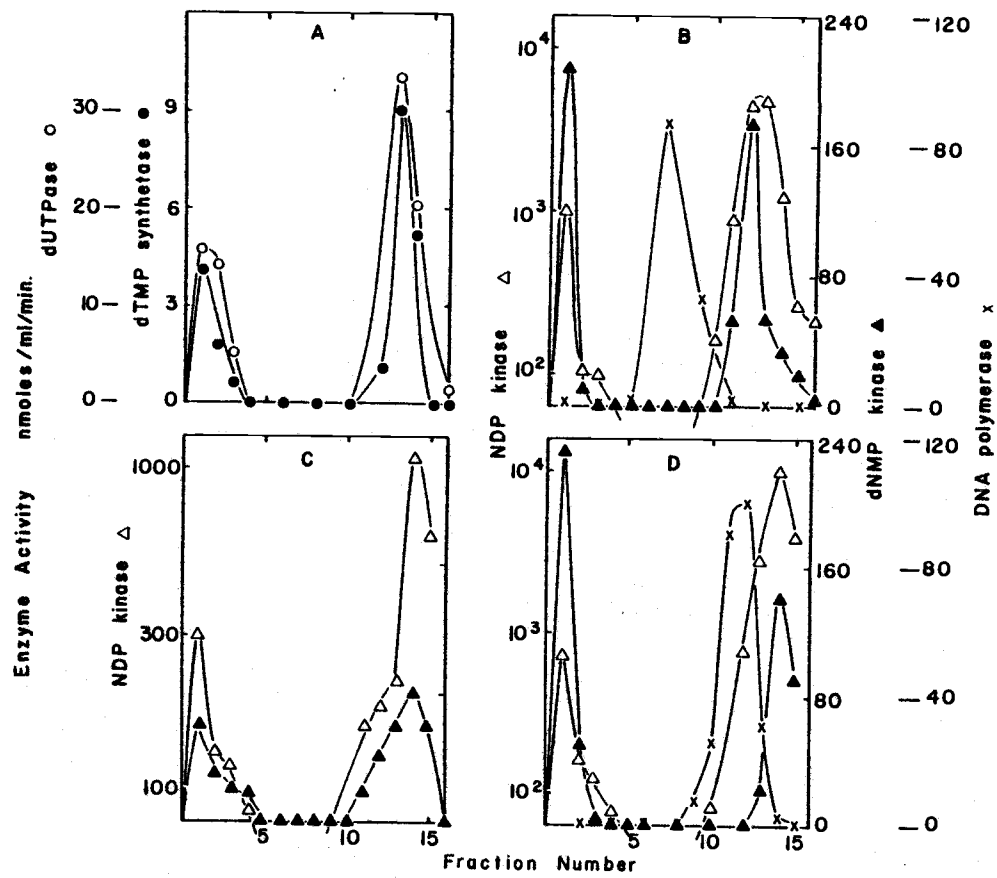


Figure 6. Sedimentation analysis of enzyme activities in a crude extract of T4-infected *E. coli* B. Sedimentation is from right to left. From G.P.V. Reddy, Thesis (1978) University of Arizona.

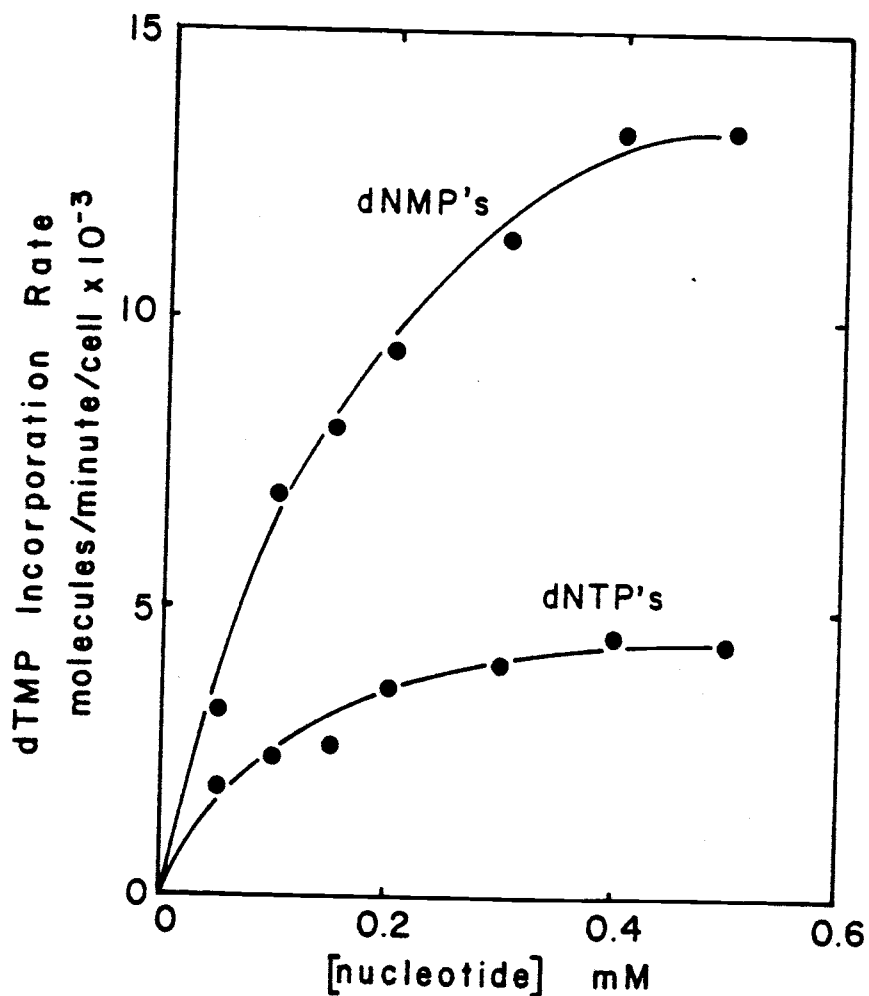


Figure 7. Deoxynucleotide incorporation in situ at different concentrations. All four deoxynucleotides were present at each indicated concentration on the figure. 'in situ' means in sucrose treated or 'plasmolysed' cells. From Reddy et. al. (1978),

Mathews 1978). The third consists of in vitro 'kinetic coupling' data showing that a rapidly sedimenting aggregate of dNTP synthesizing enzymes forms more end-product of a multistep reaction with a lower concentration of intermediates than would be expected for uncomplexed enzymes under identical conditions, Fig. 8 (Reddy et al 1977; Allen et al 1983).

PRESENT WORK

The results presented in this dissertation demonstrate that the above data are consistent with simpler interpretations than that of a dNTP synthesizing multi-enzyme complex in vitro and/or in situ . Alternative explanations also have been considered for some previously published data on in vivo complex but are not presented in this thesis. This material has not been included because I have not performed experiments to test their validity. However, the three primary lines of in vitro and in situ evidence are considered here. None of the results presented in this thesis have been published previously.

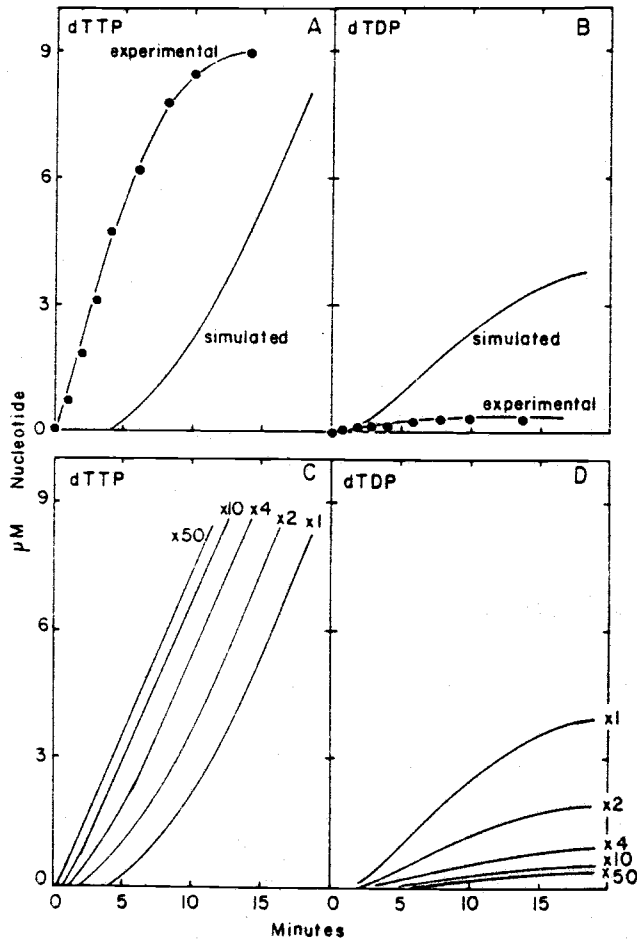


Figure 8. Production of dTTP from dTDP by aggregated enzymes. (A and B) Experimental data, along with simulated results which would have been expected if the enzymes involved were not kinetically linked. (C and D) Simulations based upon increases in concentrations of intermediates by arbitrary factors of 2, 4, 10, and 50. From Bacteriophage T4 (1983) American Society for Microbiology, Wash. D.C.

II. MATERIALS AND METHODS

Phage, Bacteria, and Culture Conditions

Experiments on rapidly sedimenting enzyme aggregates were performed with E.coli 201, a host strain lacking thymidylate synthase, and T4 sp62am N82 (reg A-, 44-), a phage strain with a DNA-negative phenotype selected for its induction of high levels of early phage enzymes. In separate experiments (by Dr. Christopher Mathews) it was found that this double mutant can form a kinetically coupled enzyme aggregate after infection, of the kind described by Allen et al (1983). For purification of T4 thymidylate synthase and for experiments on aggregated thymidylate synthase formed in the absence of other T4 proteins I used E. coli MB151, a strain carrying a high-expression plasmid vector into which had been cloned a T4 DNA fragment carrying the td gene, which encodes thymidylate synthase. This strain, which was constructed and described by Belfort et al (1983), was kindly provided by Dr. Marlene Belfort (New York State Department of Health).

Phage-infected bacteria were prepared in quantity by growth of the bacteria in a New Brunswick Micro-Ferm fermentor. Infection was carried out, when the bacteria had reached a cell density of about 4×10^8 /ml, at a multiplicity of 5 phage per bacterium. Cells were harvested at 15 minutes after infection and stored at -80 degrees C, from which they could be thawed and extracted without loss

of enzyme activity. Extraction involved resuspension in HEK buffer (25mM HEPES buffer, pH 7.6, 0.1 mM EGTA, 2 mM B-mercaptoethanol, 50 mM KCl), followed either by brief sonic oscillation or by lysozyme lysis. The latter involved treatment for one hour at 0 degrees C with 10 μ g of T4 lysozyme per gram of infected cells, followed by one cycle of freeze-thawing in liquid nitrogen. The T4 lysozyme was kindly provided by Dr. Brian W. Matthews (University of Oregon). In either case the lysates were clarified by centrifugation for ten minutes at 27,000 x g. Sedimentation profiles of thymidylate synthase activity were essentially identical with either method.

Isoelectric Focusing This was performed in a bed of IEF-Sephadex beads (Pharmacia), using ampholytes from either Pharmacia or Bio-Rad. The beads allow large aggregates to migrate through the support matrix. Samples were applied along most of the bed length, except near the electrodes at each end. Focusing was carried out at low voltage (500-1000 v) and over a period of at least six hours, to prevent disaggregation. pH values were determined by applying a flat pH electrode to the bed after focusing. Fractions were obtained by scooping up equal sections of the beads and suspending each in buffer. Each fraction was assayed directly for enzyme activity, once the beads had been allowed to settle. pI values for purified proteins were determined both in a bead matrix and in agarose gel

beds, with the use of standard protein markers (FMC Corp.).

Purification of Thymidylate Synthase For the isoelectric focusing experiments homogeneous T4 thymidylate synthase was kindly provided by Dr. Gladys F. Maley (New York State Dept. of Health). For later experiments I purified the enzyme myself, starting with the overproducing strain, E. coli MB151 (see above). The purification procedure was that of Plante et al (1978). The key step in this procedure is affinity chromatography on a column of N α -[pteroyltetra(γ -glutamyl)]-lysine, which was kindly provided by Dr. Roy L. Kisliuk (Tufts University). Based upon the specific activity reported for homogeneous T2 thymidylate synthase of 15 μ moles/min/mg protein at 30 °C (Galivan et al 1974), I estimate my preparations (8 μ moles/min/mg at 20 C) to be more than 50% pure with no contaminating phage protein present. Purified Lactobacillus casei thymidylate synthase was kindly provided by Denice Mittelstaedt and Dr. Michael Schimerlik of this department.

Purification of dCMP Hydroxymethylase Homogeneous
dCMP Hydroxymethylase was purified by starting with a frozen stock of T4 sp 62 am N82-infected E. coli 201. Separation of thymidylate synthase and dCMP hydroxymethylase was achieved with the use of a DEAE-Sepharose column. The final (and novel) purification step was adapted from that of Plante et al for the

proportional to the volume pumped out of the gradient. Sedimentation is from left to right in all profiles depicted unless otherwise stated. Enzyme assays were as described in previous publications from this laboratory (Reddy and Mathews 1978, Reddy et al 1977, Allen et al 1980).

Nucleic Acids Purified E. coli ribosomal RNA was provided by Dr. Henry Schaup of this department, and purified M13 phage DNA was a gift of Kuan-chih Chow of this department. Purified pBR322 plasmid DNA was provided by Joseph Booth of this laboratory. Synthetic ribo- and deoxyribo-homopolymers were purchased from P-L Biochemicals.

¹⁴C Labeling of Early Phage Enzymes 50 ml of E. coli B was grown to a density of 3×10^8 cells/ml at 37°. The cells were transferred to a Petri dish with spin bar and irradiated with constant stirring for 13 minutes at a distance of 6 inches from a model UVS 54 (254 nm) light source. The cells were maintained in the dark with agitation for an additional 10 minutes. The cells were then chilled on ice and infected with a multiplicity of infection of 10 with T4D. ¹⁴C labeled amino acids were added to make a final specific activity of 2 μ C/ml of medium and the culture was transferred to a 37° water bath for 8 minutes. The labeling was chased with 10 ml of a stock

solution of cold casamino acids and the cells were chilled on ice. The cells were pelleted and resuspended in M9 buffer. The cells were sonicated and the lysate centrifuged to remove the membrane fraction. A 20- μ l aliquot of the extract contained 233,840 cpm while the acid precipitate contained 199,150 cpm. M9 buffer for this experiment contained 6.0 g Na_2HPO_4 , 30 g K_2PO_4 , 1.0 g NH_4Cl , 0.2 g $\text{MgSO}_4 \cdot 7\text{H}_2\text{O}$, 0.01 g CaCl_2 per liter.

Binding Purified Proteins to Affi-Gel Matrix

Proteins to be bound were dialyzed into HEPES buffer which contained no mercaptans or amines (B-mercaptoethanol or Tris), as these react with the activated matrix. The Affi-Gel was washed with cold deionized water to remove the stabilizing solvent, isopropyl alcohol. The buffered protein solution was then added to the gel and gently agitated overnight at 4°C. Any activated gel left after agitation was neutralized by passing buffer containing 2 mM B-mercaptoethanol through the column. Buffer containing 1 molar NaCl was used to wash unbound protein from the column. Column effluent was assayed for protein to assess the efficiency of binding. The procedure was essentially the same as that of Formosa and Alberts (1983).

5' Nucleotidase Assays

Two nucleotidase assays are mentioned in the RESULTS section. The reaction conditions and chromatography were the same as for the coupled

activity assay of Reddy et al 1977. However, the usual folate and nucleotide substrates were omitted. The two labeled substrates, dTTP and ATP, can be used interchangeably due to a lack of enzyme substrate specificity (Neu, 1967). The dTTP was labeled with tritium on the methyl group at the 5 position. Final specific activity was 2.5 CPM/ nanomole of dTTP. Activity in a crude extract of T4-infected cells is 33 nanomoles per min. per ml. of extract. This activity agreed fairly well with that published by Neu. Gamma labeled ^{32}P ATP was used when sucrose gradient fractions were assayed. Release of the labeled terminal phosphate was measured by specific binding of the nucleotide to activated charcoal (Norite). Since the released phosphate is not bound, the added charcoal was pelleted and the supernatant was counted in the liquid scintillation counter. Thus, this second assay requires no chromatographic separation of labeled nucleotides as with the one used above. I adapted this procedure from the tritium release assay for thymidylate synthase developed in Greenberg's laboratory.

Computer Simulations of Coupled Activity

Gerry

Lasser and I developed a Fortran IV program to simulate the concentration of nucleotide intermediates and final product for the coupled assay described by Reddy et al 1977. The enzymes were assumed to be uncomplexed and to obey the steady state equations also used by Reddy et al 1977. The

Abbreviations Used

Table 2 is a general listing of the abbreviations used throughout this dissertation.

Table 2. List of abbreviations

<u>Abbreviation</u>	<u>Meaning</u>
<u>am</u>	amber
CPM	radioactive counts per minute
dNMP	deoxyribonucleoside monophosphate
dNDP	deoxyribonucleoside diphosphate
dNTP	deoxyribonucleoside triphosphate
DA	DNA-arrest
DD	DNA-delay
DO	DNA-negative
EGTA	[Ethylenebis(oxyethylene nitrilo)] tetraacetic acid
FH2	dihydrofolate
FH4	tetrahydrofolate
HEPES	N-2-Hydroxyethylpiperazine N'-2-ethanesulfonic acid
hm-dCMP	5-hydroxymethyldeoxycytidine monophosphate
hm-dCDP	5-hydroxymethyldeoxycytidine diphosphate
hm-dCTP	5-hydroxymethyldeoxycytidine triphosphate
P (followed by a number)	product of the gene to which the number refers
rNDP	ribonucleoside diphosphate
T4	T4 Bacteriophage

III. RESULTS

Part 1: T4 Thymidylate Synthase Binds Nucleic Acid

Isoelectric focusing of a multienzyme aggregate

Isoelectric focusing was used in an attempt to augment various procedures previously reported by this laboratory for the partial purification of the proposed dNTP-synthesizing enzyme complex (Reddy et al 1977; Allen et al 1980, 1983). A crude extract of T4-infected cells was focused in a matrix of Sephadex beads and is depicted in Figure 9. Three phage enzymes -- thymidylate synthase, dNMP kinase, and dihydrofolate reductase -- focused in a broad band between pH 3 and 5, with distinct peaks near pH 4.0 and 4.9. The host enzyme, nucleoside diphosphate kinase, focused with a maximum near pH 4.7, a value identical to that I have determined for the enzyme purified by Gerry Lasser. Dihydrofolate reductase, also purified by Gerry Lasser, has a pI of about 5.1, which is nearly the same as that shown in Figure 9. However, purified T4 thymidylate synthase has a pI of 7.1-7.3 (determined by myself and personal communication from Dr. Gladys F. Maley), which is not in agreement with the crude extract profile. This result supports the notion that the enzyme in a crude extract is physically associated with a particle of large buffering capacity with a pI of 4.0 to 5.0.

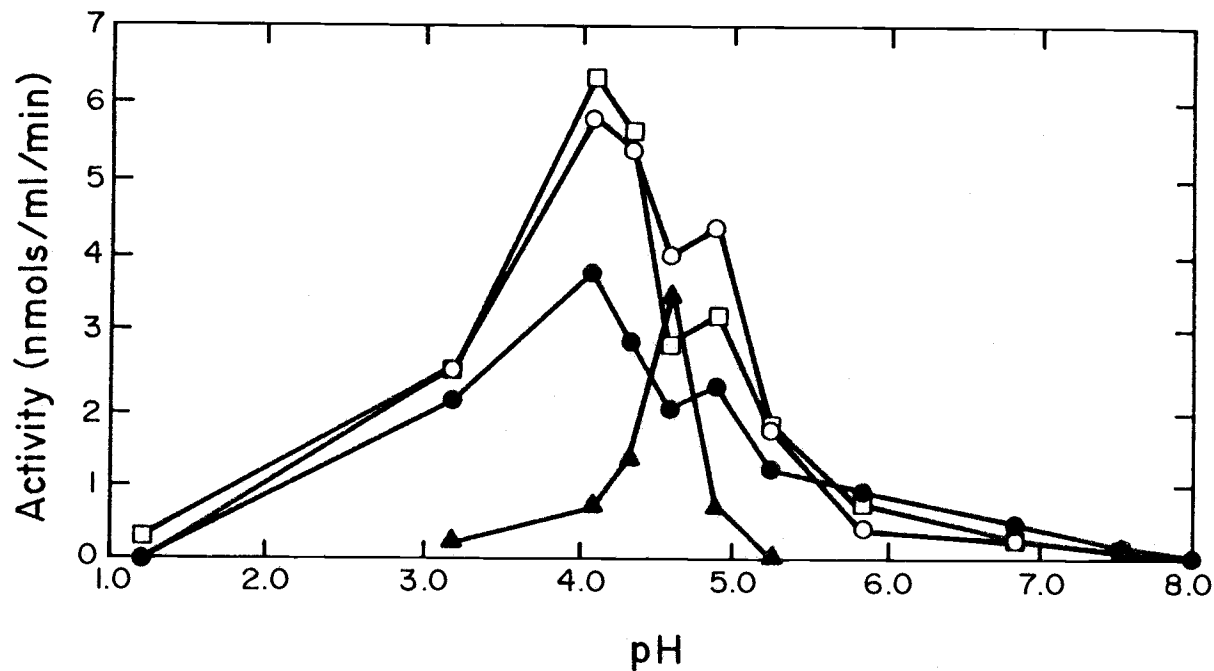


Figure 9. Isoelectric focusing of activities in an extract of phage-infected *E. coli* 201. Focusing was carried out in a Sephadex medium, as described in Materials and Methods. Recovery of each activity assayed was about 90%. ●, Thymidylate synthase; ◻, dihydrofolate reductase; ○, deoxyribonucleoside monophosphokinase x 0.1; ▲, nucleoside diphosphokinase x 0.001.

Kinetic coupling in aggregated thymidylate synthase

While experimenting with different fractionating techniques for the enzyme aggregate, Joe Booth of this laboratory found that several dNTP-synthesizing enzyme activities coprecipitate at 30-50% saturation of ammonium sulfate (Allen et al 1983). To further assess the possible linkage of these enzymes, I sedimented a redissolved pellet through a sucrose gradient, as depicted in Fig. 10. About half of the thymidylate synthase activity sedimented rapidly, but the proportion of other rapidly-sedimenting enzyme activities was low, as judged by the spectrophotometric assay for the conversion of dCTP to dTMP. This assay monitors the last step of the catalytic series: $dCTP \rightarrow dCMP \rightarrow dUMP \rightarrow dTMP$. The gradient absorbance profile shown in Fig. 10 suggested that the aggregated thymidylate synthase and small amount of other aggregated enzymes were cosedimenting with UV light-absorbing material. A wavelength scan of fractions 5 and 6 (data not shown) revealed in each case a maximum at 258 nm with a 260/280 ratio of 1.8. These values indicate the presence of both nucleic acid and protein, suggesting the possible presence of ribosomes. Since the cells were infected with a T4 phage mutant unable to synthesize DNA (D0 mutant) but with the wild type ability to break down host DNA, the nucleic acid detected above is probably rRNA. Sedimentation of crude extracts by other investigators shows the same type of ribosome profile, Tissieres (1974)

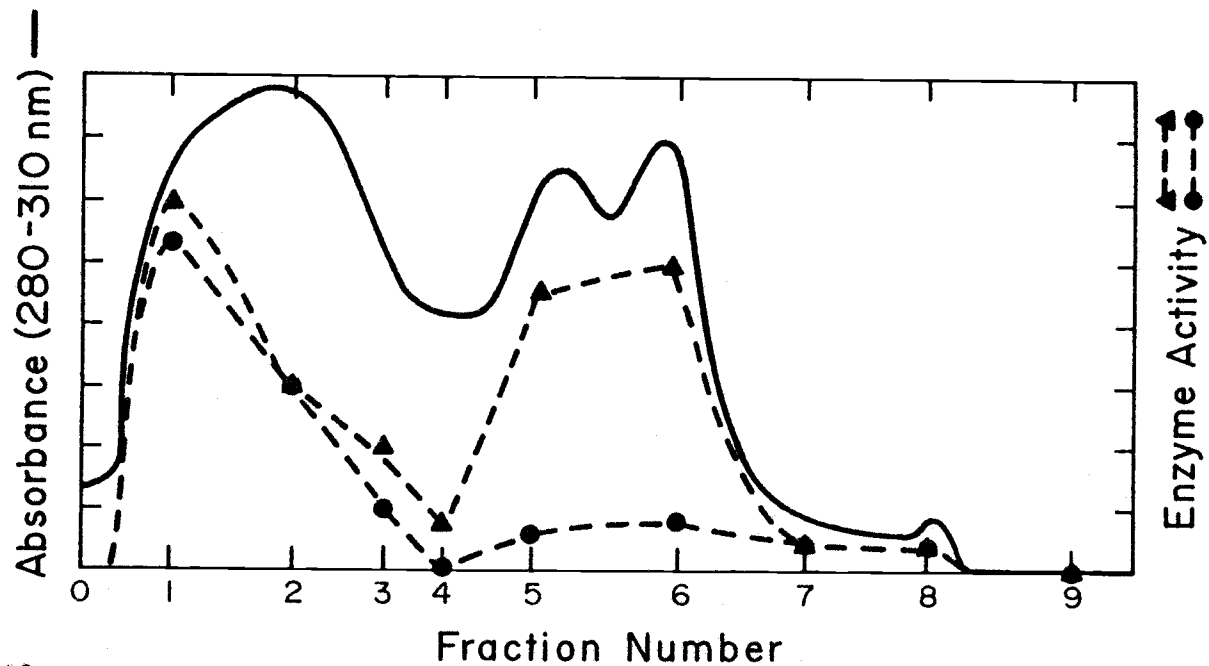


Figure 10. Sedimentation profile of activities in a 30-50% ammonium sulfate precipitate from a crude extract of T4-infected *E. coli*. The precipitate was dissolved in HEK buffer, dialyzed, and an aliquot layered on a 10-50% sucrose gradient, as described in Materials and Methods. After centrifugation, the gradient was fractionated with continuous monitoring of ultraviolet absorbance (solid line). Fractions of unequal volume were collected and assayed for thymidylate synthase (▲) and the coupled sequence dCTP → dCMP → dUMP → dTMP. Sedimentation is from left to right.

notes:

"... an important paper was published by Schachman, Pardee, and Stanier (1952). They showed that when bacterial extracts prepared in 0.02-0.05 M NaCl are examined in the analytical centrifuge, three principal components forming very sharp boundaries are found with uncorrected sedimentation coefficients of about 40S, 29S, 5S. It should be noted that no magnesium was added to these extracts. The same type of pattern was obtained from a number of bacterial species and from extracts made by breaking the cells in different ways. These components were shown to comprise the bulk of the cellular RNA, and the 40S peak contained 40% RNA and appeared in the electron microscope as spherical particles (Luria et al. 1943).".

The buffer salt composition stated above is identical to that used in this laboratory. Since ribosomes comprise 30% of the bacterial cell mass, the peak size, location, and absorbance ratio provide evidence that dNTP-synthesizing enzymes are cosedimenting with ribosomal subunits.

The effect of Mg⁺⁺ and its reversibility

The rapidly sedimenting forms of T4 thymidylate synthase are disaggregated by Mg⁺⁺ ion (Reddy and Mathews,

1978; and unpublished results). Also, ribosomal subunit association is sensitive to Mg^{++} concentration. This, to me, suggested that disaggregation of ribosomes in low Mg^{++} might expose a binding surface to which thymidylate synthase could become attached. To approach this question I first asked whether the disaggregation of thymidylate synthase in low Mg^{++} is reversible (Fig. 11). A crude extract of infected cells was centrifuged in 10 mM Mg^{++} , which caused thymidylate synthase to sediment as the free enzyme. Fraction 2 from this gradient, which contains the free enzyme, and fraction 7, which contains ribosomes (as determined by sedimentation position), were combined, dialyzed, and resedimented in a magnesium-free gradient, whereupon all of the enzyme became aggregated (panel B).

Sensitivity of aggregation to monovalent cations

To further characterize the nature of this aggregation I sedimented a crude extract of infected cells through sucrose gradients containing varying concentrations of KCl (Fig. 12). Little or no aggregation was seen above 50 mM KCl.

Effect of substrates upon enzyme aggregation

The possible binding of T4 thymidylate synthase to E. coli ribosomes could be due to interaction with either protein or rRNA. To test whether this interaction was via the enzyme substrate- or cofactor-binding sites,

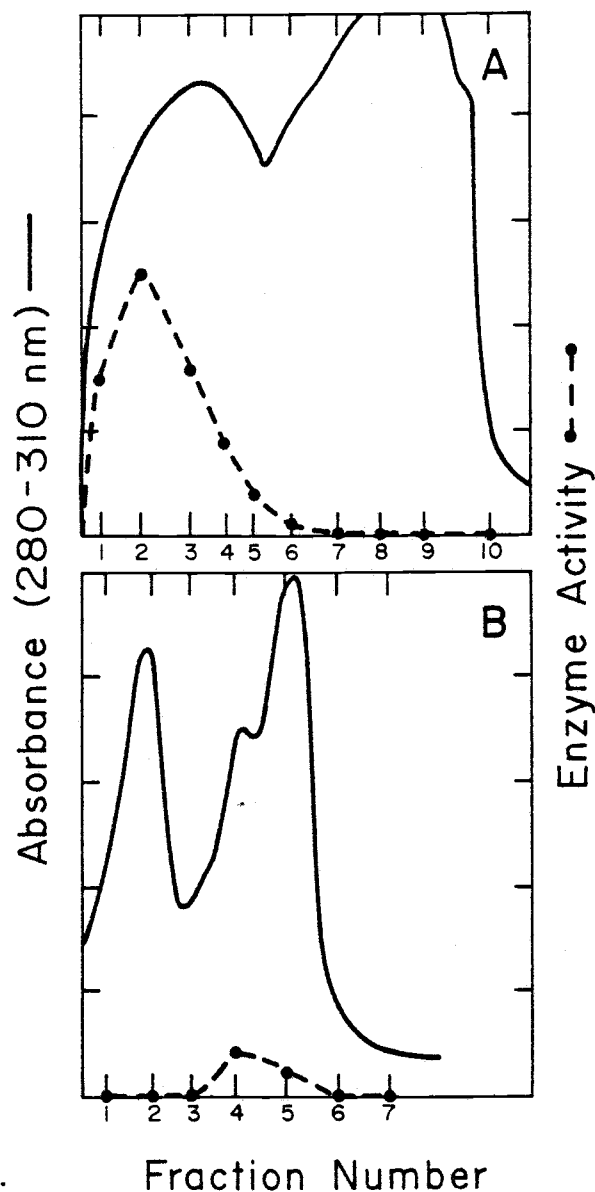


Figure 11. Effect of Mg^{++} upon sedimentation of thymidylate synthase. Panel A depicts sedimentation of a crude infected cell extract through a sucrose gradient in which the sucrose solutions contained 10 mM $MgCl_2$. Fractions 2 and 7 were combined, dialyzed in magnesium-free HEK buffer, and resedimented in the absence of Mg^{++} . Panel B depicts the resedimentation profile. Each tick on the ordinate represents 5 nmoles/min/ml fraction. Sedimentation is left to right.

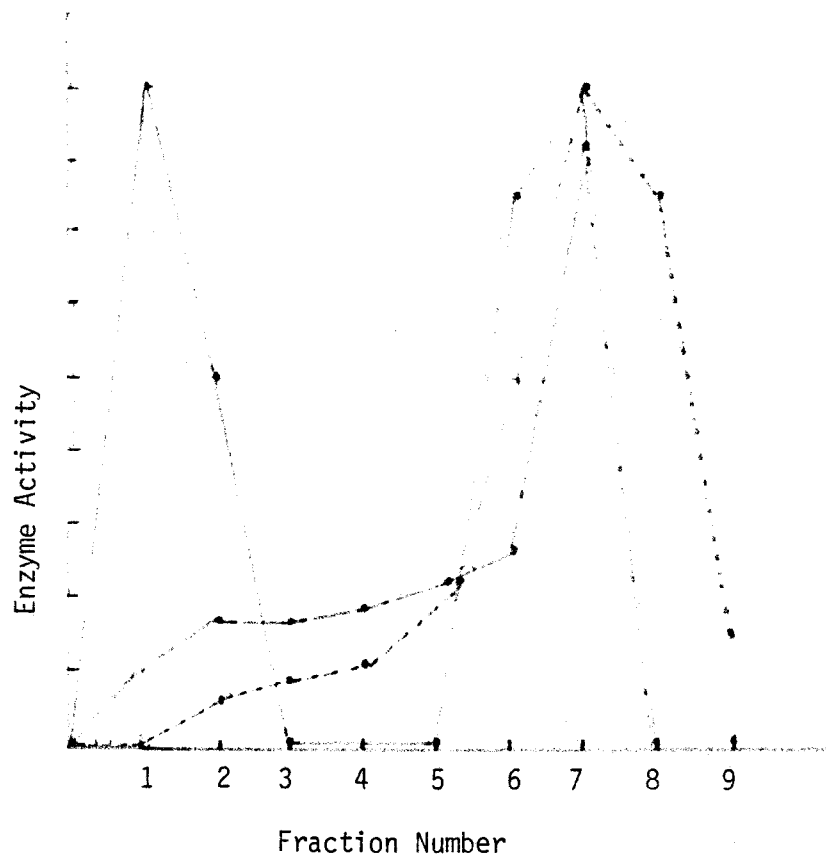


Figure 12. Effect of K^+ upon sedimentation of thymidylate synthase. Sedimentation is from right to left. Each tick on the ordinate represents 2 nmoles/min/ml fraction. A crude cell extract was sedimented through a 5-25% sucrose gradient containing a one-ml 66% sucrose shelf as used by Reddy *et al* (1977). KCl concentrations were as follows: 50 mM (—); 100 mM (— — —); 150 mM (- - - -).

competitive binding assays were performed. As shown in Fig. 13, 2 mM dUMP had no effect on the sedimentation profile (panel B), but 0.2 mM methylenetetrahydrofolate abolished rapid sedimentation (panel C). The assay buffer used for all kinetic coupling assays, which includes Mg^{++} and methylenetetrahydrofolate, also abolished aggregation (panel D). The off-scale absorbance profile in 13 B, C, and D was due to the large extinction coefficients for the added dUMP and methylenetetrahydrofolate. Later I found that methylenetetrahydrofolate also disrupted complexes between purified thymidylate synthase and nucleic acids as seen in Figure 14.

Aggregation of T4 thymidylate synthase in the absence of other phage proteins

The above experiments show that T4 thymidylate synthase becomes disaggregated when either of its two cofactors (Mg^{++} and FH_4) are present. This suggests that aggregation may be a property solely of the enzyme and independent of its associations with other phage proteins. To test this idea, I took advantage of a recombinant plasmid (Belfort et al 1983), in which synthesis of T4 thymidylate synthase from its cloned structural gene is put under the control of a thermolabile λ phage c_{I} repressor. The cloned T4 DNA segment in this plasmid (2.7 kb) contains 0.4 kb at the 5' end of the dihydrofolate reductase coding region (Maley et al 1979), the 0.8-kb coding region for thymidylate

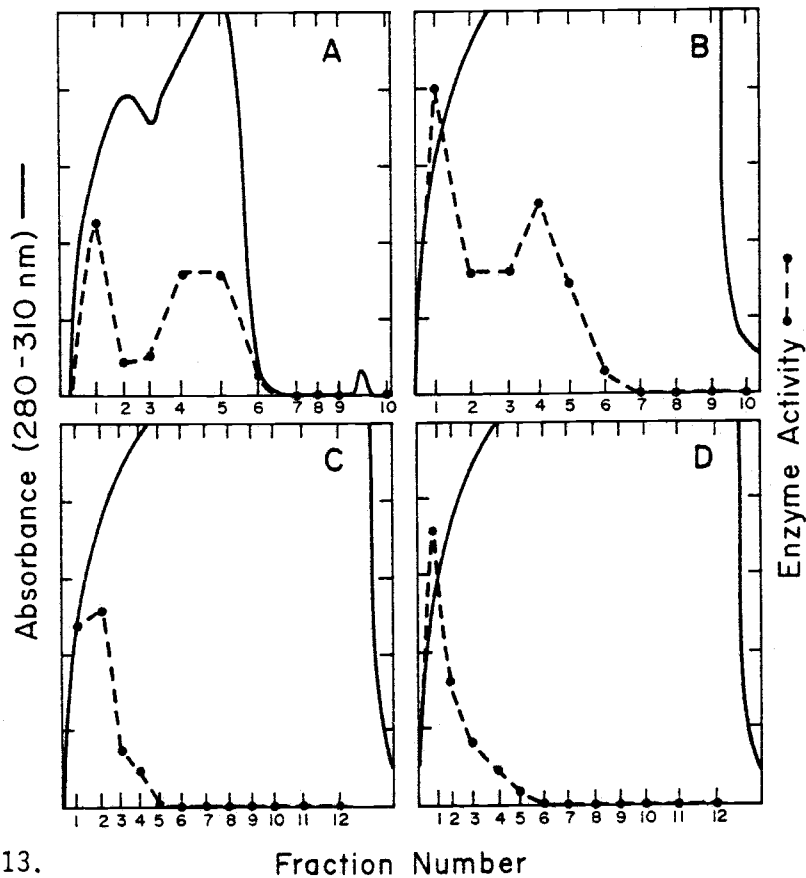


Figure 13. Fraction Number

Effects of substrates upon sedimentation of T4 thymidylate synthase. Conditions of cell lysis and centrifugation are as described in Materials and Methods and the legend to Fig. 2. Additions to the sucrose solutions used to prepare the gradients: A, none; B, 2 mM dUMP; C, 2 mM dUMP plus 0.2 mM methylenetetrahydrofolate. In D the sucrose solutions were not in HEK buffer, but in thymidylate synthase assay reagent: 0.1 M Tris-HCl, pH 7.4, 0.1 M KCl, 0.1 M β -mercaptoethanol, 0.025 M $MgCl_2$, 0.015 M formaldehyde, and 2 mM dUMP. Each tick on the ordinate represents 5 nmoles/min/ml fraction.

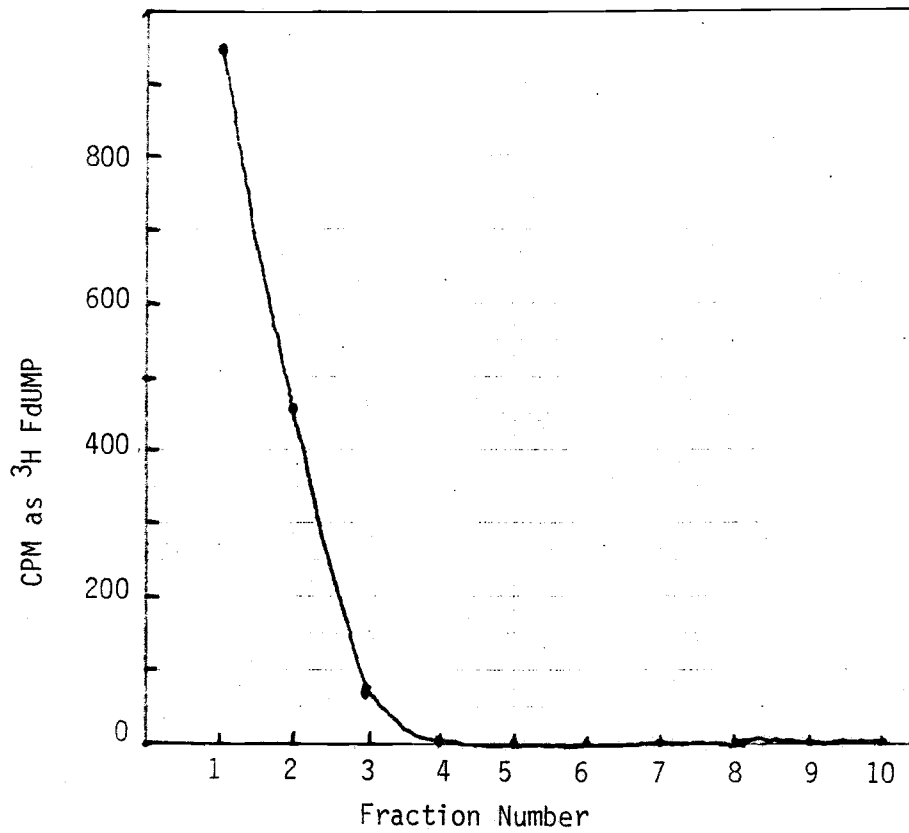


Figure 14. Sedimentation profile of a mixture of ³H FdUMP + CH₂FH₄ + thymidylate synthase + rRNA. Conditions were the same as Figure 17 except that sedimentation was at 30,000 instead of 24,000 rpm. Sedimentation from left to right.

synthase, and the recently described 1.0-kb intron in the gene for thymidylate synthase (Chu et al 1984). No other complete T4 proteins are expressed from the cloned fragment other than thymidylate synthase. E. coli MB151, which carries this plasmid, was grown at 32 and then incubated at 43 , to allow synthesis of T4 thymidylate synthase. As shown in Fig. 15, cells were lysed and the lysates sedimented as described earlier. Enzyme sedimentation profiles were quite similar to those seen with infected cells (Figs. 11 and 13); about half of the enzyme sedimented rapidly in the absence of Mg⁺⁺ but not in its presence at 10 mM. Thus, the enzyme can aggregate independently of any associations with other T4 proteins.

Associations of purified T4 thymidylate synthase with nucleic acid

Since T4 thymidylate synthase aggregates with purely cellular material and cosediments with ribosomes it seemed logical to explore these interactions with the use of purified components. A large culture of E. coli MB151 was grown and then incubated at a higher temperature, for increased production of T4 thymidylate synthase. The enzyme was purified to greater than 50% homogeneity as judged by the specific activity as compared with the purified T2 enzyme. I then performed a series of experiments in which the sedimentation behavior of the enzyme was analyzed after incubation with various nucleic acids. The first experiment

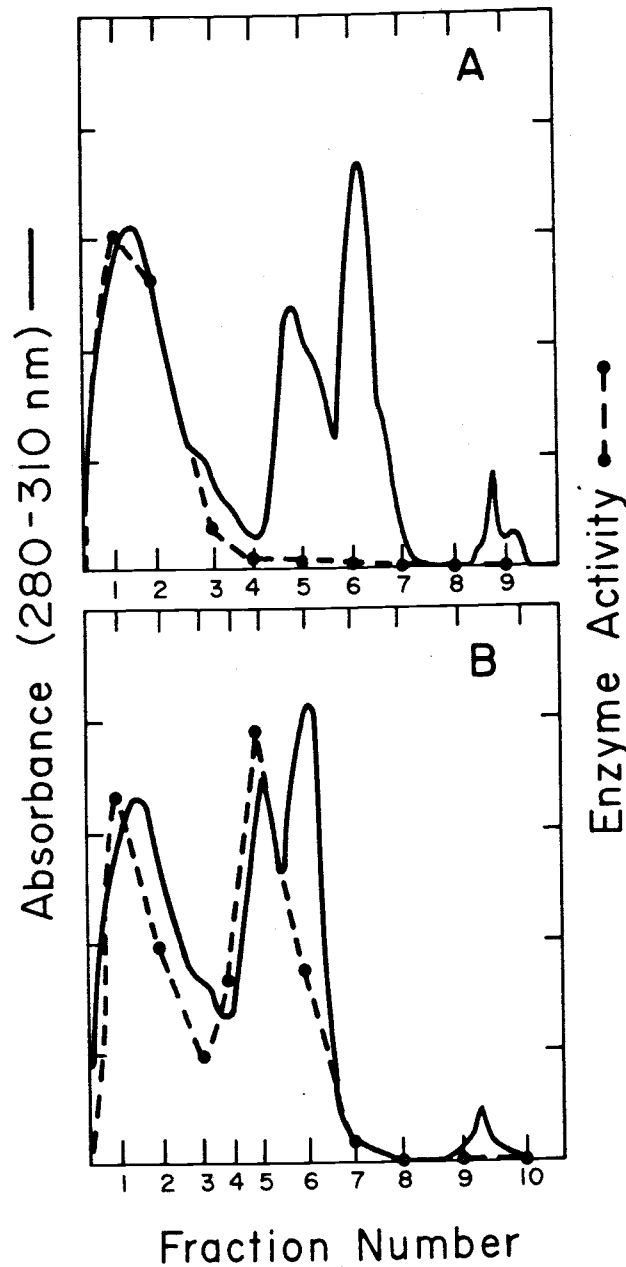


Figure 15.

Sedimentation profile of T4 thymidylate synthase expressed from the *td* gene cloned into a high-expression plasmid vector. A lysate of *E. coli* MB151 was sedimented through sucrose gradients containing 10 mM MgCl₂ (panel A) or no MgCl₂ (panel B). Each tick on the ordinate represents 5 nmoles/min/ml fraction. (Left to Right)

(Fig. 16) involved thymidylate synthase and single-stranded DNA, isolated from M13 phage. The enzyme did bind to this DNA, as shown by cosedimentation, and the binding was sensitive to Mg^{++} at 10 mM (panel B). The ability to bind DNA tightly seems to be a distinctive property of the T4 enzyme, for purified L. casei thymidylate synthase showed very little binding when treated identically to the T4 enzyme (compare panels A and C).

Next I asked whether T4 thymidylate synthase could associate with double-stranded DNA, using plasmid pBR322 as the source of this material. The data of Fig. 17 indicate that no binding occurred to either the superhelical or the relaxed forms of the plasmid, or in the presence or absence of Mg^{++} .

Since this investigation started with the observation that T4 thymidylate synthase might be binding to ribosomes, I wanted to know whether the enzyme would bind to purified ribosomal RNA. Those results, shown in Fig. 18, are virtually identical to those seen with M13 DNA; all of the enzyme in the incubation mixture bound to the rRNA in the absence of Mg^{++} , while none bound in the presence of 10 mM Mg^{++} .

All of these data suggest that T4 thymidylate synthase binds rather nonspecifically to either DNA or RNA, with the provisos being that the nucleic acid must be single stranded and that sub-physiological cation concentrations be present. In accordance with this idea, I found that the

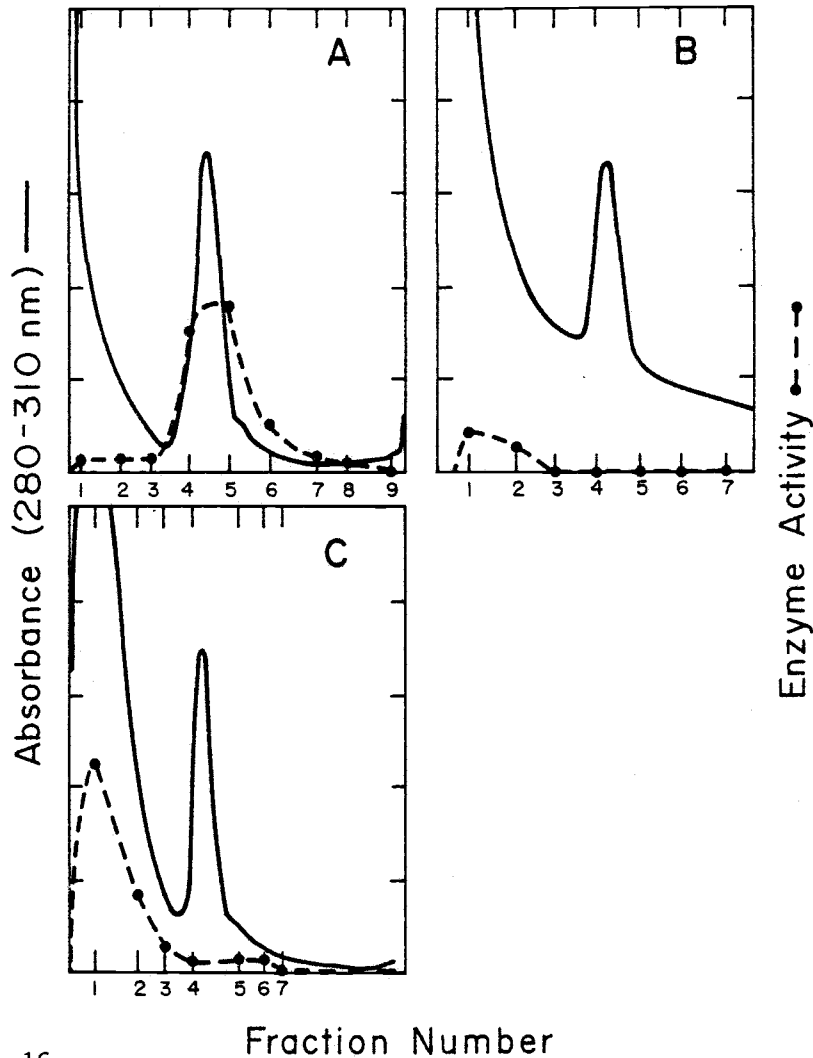


Figure 16.

Binding of T4 thymidylate synthase to single-stranded DNA. A, purified T4 thymidylate synthase (about 2 μg) was mixed with 1 A_{260} unit of M13 phage DNA and the mixture was immediately sedimented through a sucrose gradient containing no Mg^{++} . B, identical to A except that somewhat less enzyme was used, and the sucrose gradient solutions contained 10 mM MgCl_2 . C, identical to A except that *L. casei* thymidylate synthase was used instead of the T4 enzyme. Each tick on the ordinate represents 5 nmoles/min/ml fraction. (Left to Right)

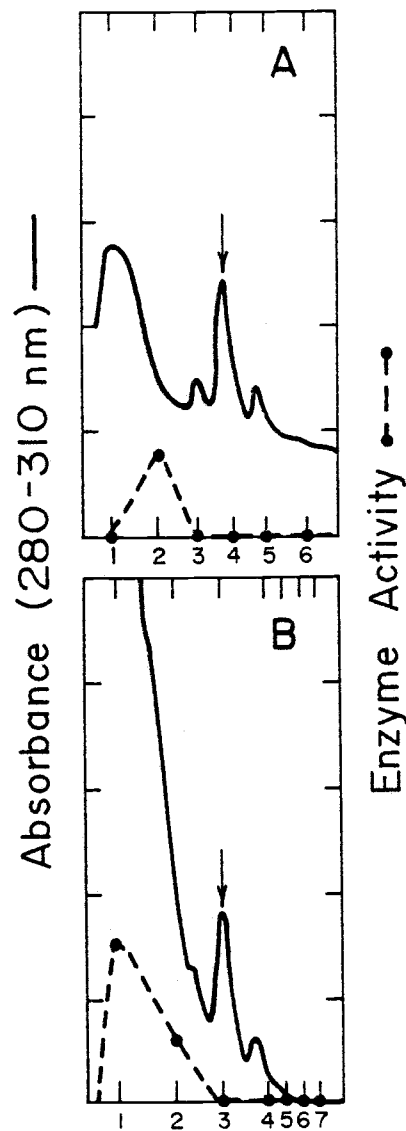


Figure 17.

Fraction Number

Lack of binding of thymidylate synthase to double-stranded DNA. Conditions were identical to those described in Fig. 16, except that pBR322 plasmid DNA was used instead of M13 DNA. Sedimentations were carried out in the absence of Mg^{++} . The arrows point to the major peak of DNA (presumably superhelical monomers) and hence identify where thymidylate synthase activity would have been seen had it bound. A, T4 enzyme; B, *L. casei* enzyme. Each tick on the ordinate represents 5 nmoles/min/ml fraction.

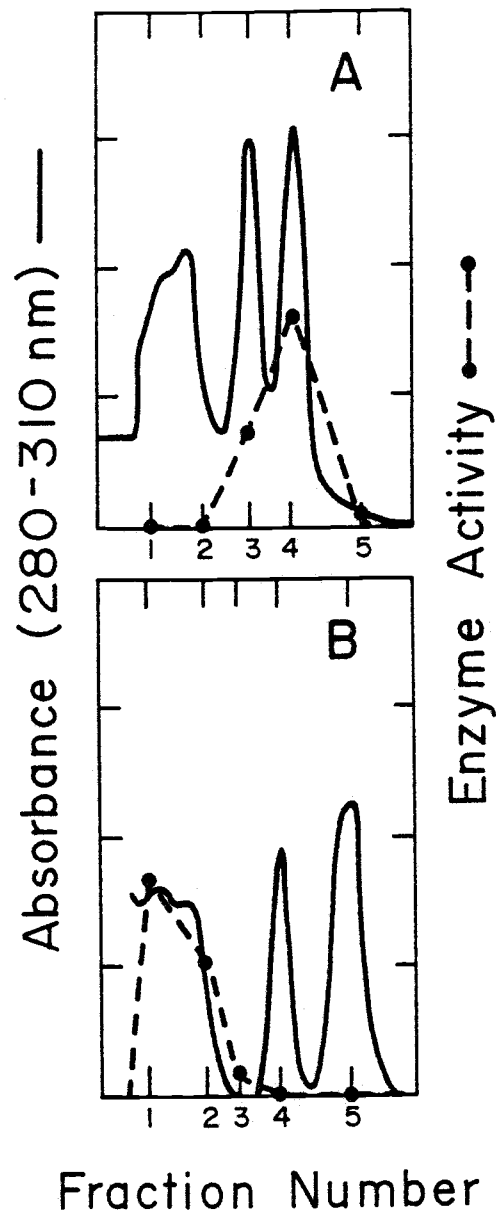


Figure 18.

Binding of T4 thymidylate synthase to purified *E. coli* rRNA. Conditions are the same as in Fig. 16 except for the use of *E. coli* rRNA instead of M13 DNA. A, sedimentations run in the absence of Mg^{++} ; B, 10 mM Mg^{++} present in the sucrose solutions. Each tick on the ordinate represents 5 nmoles/min/ml fraction.

enzyme also binds to synthetic homopolymers, either poly(A) or poly(U), in the absence of Mg^{++} (Fig. 19). Note that because of the relatively small size of the polymers, the enzyme-polynucleotide complexes sedimented somewhat faster than the free polynucleotides. However, the increased rate of sedimentation is not great enough to suggest the possibility of the cooperative binding seen with T4 gene 32 protein. Similar results were seen with the deoxyribohomopolymers poly(dA) and poly(dT) (data not shown).

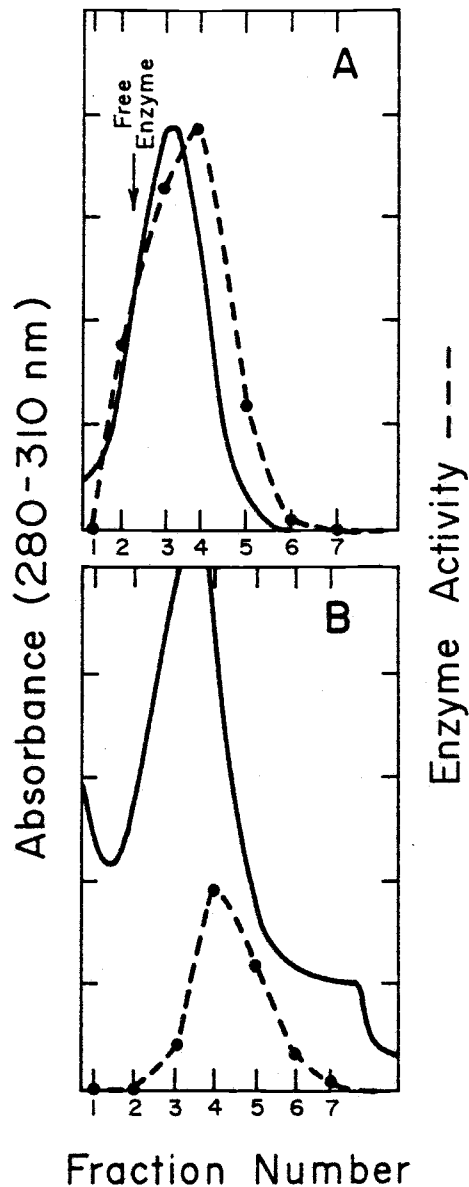


Figure 19.

Binding of T4 thymidylate synthase to nucleic acid homopolymers: either poly A (6-13S), panel A; or poly U (5-12S), panel B.

Conditions are as described in Fig. 16. Mg^{++} was absent in both sedimentations. The arrow shows where free enzyme would be expected to sediment. Each tick on the ordinate represents 5 nmoles/min/ml fraction. Sedimentation in this experiment was carried out in a vertical rotor, for 2 hours, at 50,000 rpm.

PART 2: Conditions for Aggregation of Other dNTP
Synthesizing Enzymes

Cation sensitivity of rapidly sedimenting protein

To see if other enzymes of the putative dNTP synthesizing complex behaved in a manner similar to that of thymidylate synthase I sedimented a crude extract through a 'low salt' (5 mM KCl, 0 mM MgCl) and a 'moderate salt' (50 mM KCl, 10 mM MgCl) sucrose gradient as shown in Figures 20 and 21. All four of the dNTP synthesizing enzymes assayed in this experiment were at least partially sensitive to a moderate salt concentration. Aggregation of thymidylate synthase and deoxynucleoside monophosphate kinase were completely eliminated while nucleoside diphosphate kinase and dCMP hydroxymethylase were partially disaggregated. Note also the relative salt-induced changes in the absorbance peak height between the slowly sedimenting low molecular weight fraction and the rapidly sedimenting ribosomal fraction. This change in distribution of total protein suggests that a variety of proteins may be aggregated with ribosomes under low salt conditions.

Host enzyme aggregation studied with uninfected cells

The possibility that rapid sedimentation is due to nonspecific aggregation was further examined by sedimenting a crude extract of uninfected cells through a 5-20% sucrose gradient containing a 0.5 ml 66% sucrose shelf at the

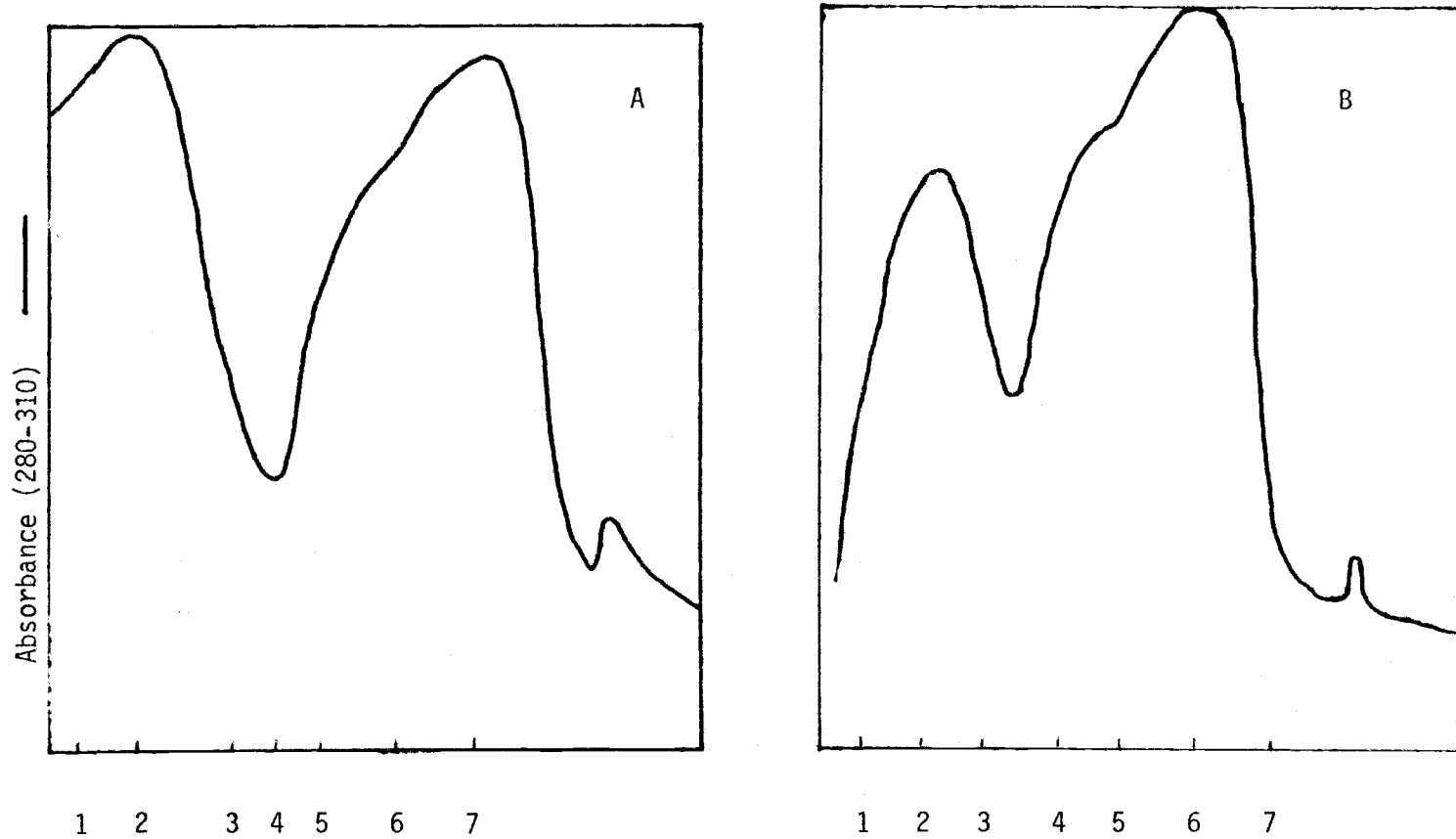


Figure 20. Effect of Mg⁺⁺ upon sedimentation of protein as estimated by A(280-310). Panel A shows effect of 10mM Mg⁺⁺. Panel B shows effect of 0mM Mg⁺⁺. Sedimentation of the crude extract is from left to right.

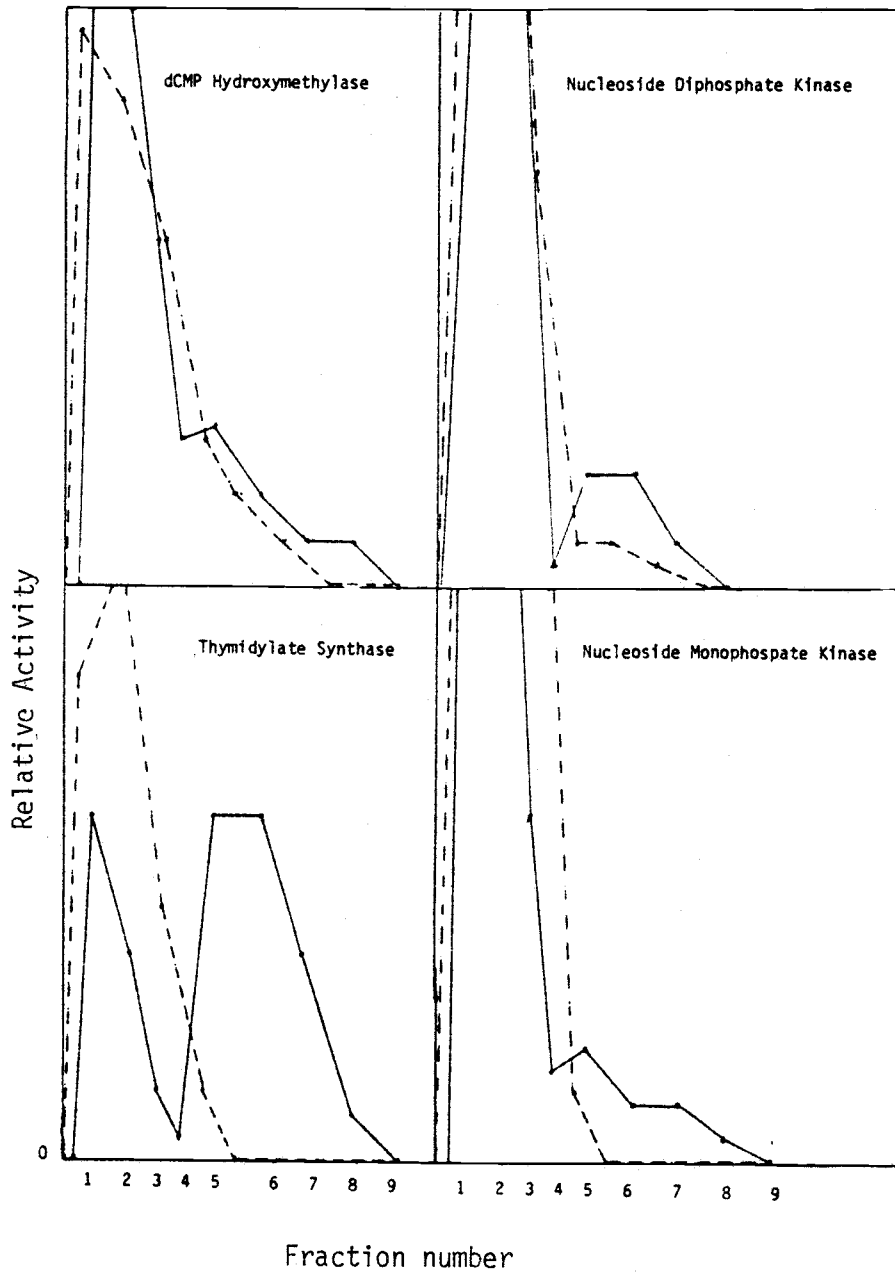


Figure 21. Individual enzyme profiles with (---) and without (—) 10mM Mg⁺⁺. Fraction numbers correspond with those of Figure 20. Activity values are only relative and can not be compared between enzyme profiles.

bottom of the tube. Experimental conditions were as used previously by Reddy et al 1977. The results, shown in Fig. 22, demonstrate that phage infection is not necessary for aggregation of host dNTP-synthesizing enzymes. This experiment clearly shows that dNTP-synthesizing enzymes in general can rapidly sediment without forming a single, specific protein-protein complex. It could be suggested that rapid sedimentation of host dNTP-synthesizing enzymes in uninfected cells may indicate the presence of a host dNTP-synthesizing complex. However, the number of replication forks per cell is about tenfold higher in infected cells (Werner, 1968) as compared with uninfected cells while the percentage of rapidly sedimenting nucleoside diphosphate kinase is, within experimental error, equivalent in both cases (compare figures 22 and 6b). This lack of correlation between the amount of rapid sedimentation and the number of replication forks per cell indicates that aggregation of dNTP synthesizing enzymes is unrelated to the replication of DNA. Such an inferred relationship has been the cornerstone of all in vitro experiments to date, including those involving coupled activity.

Non-association of purified T4 dCMP hydroxymethylase with rRNA

In order to explore the mechanism of aggregation of an additional phage dNTP-synthesizing enzyme, I purified dCMP

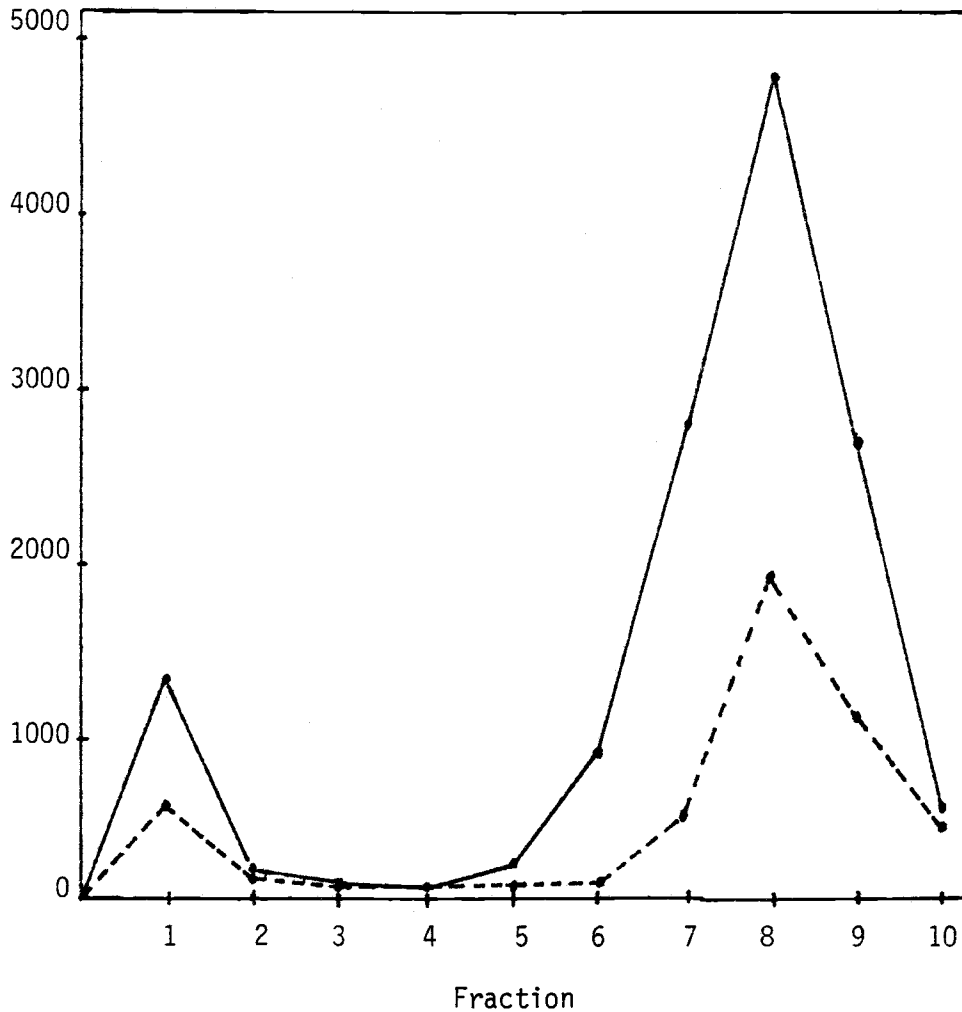


Figure 22. Enzyme activity profile of host adenylate kinase (broken line) and nucleoside diphosphate kinase (solid line) from sucrose gradient sedimentation of uninfected E. coli extract. Activity in nmoles/ml/min. Experimental details are those of Reddy et al. (1977). Nucleoside diphosphate kinase profile is identical to that reported earlier in T4 infected cells (compare with Figure 6B). Sedimentation is right to left.

hydroxymethylase to homogeneity using a new affinity purification scheme (see methods). Both thymidylate synthase and dCMP hydroxymethylase utilize methylenetetrahydrofolate as a cofactor. I reasoned that the folate analog affinity column used to purify thymidylate synthase might also bind dCMP hydroxymethylase. With a few minor procedural modifications the affinity column specifically bound the desired enzyme (Fig. 23).

A sucrose gradient centrifugation profile of a mixture of rRNA and the purified T4 dCMP hydroxymethylase, shown in Fig. 24, reveals that the enzyme does not have an affinity for rRNA under assay conditions identical to those used for T4 thymidylate synthase. This suggests that rapid sedimentation of dCMP hydroxymethylase is not due to an affinity for rRNA as is the case for T4 thymidylate synthase.

Assay for protein-protein interactions using dNTP synthesizing enzyme-bound columns

As an additional probe for evidence of a dNTP synthesizing complex, I prepared Affi-Gel purified protein columns and looked for specific protein associations using C labeled T4 phage proteins. Formosa et al. (1983) immobilized the T4 single strand binding protein, the product of gene 32, on the same agarose matrix and used it for affinity chromatography of lysates of T4-infected cells. At least 10 T4-encoded early proteins and 3 or 4

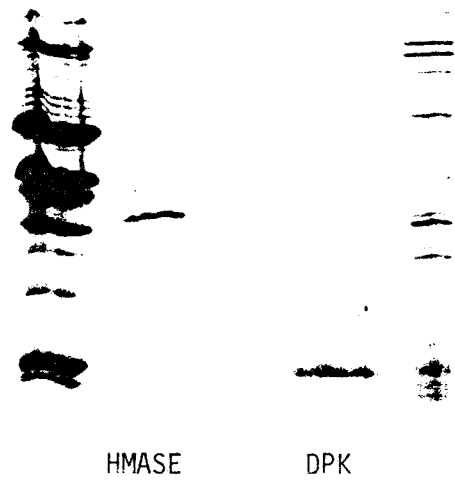


Figure 23. Polyacrylamide gel electrophoresis of purified phage dCMP hydroxymethylase and *E. coli* nucleoside diphosphate kinase. This SDS gel profile shows that the dCMP hydroxymethylase and nucleoside diphosphate kinase used in later experiments are homogeneous.

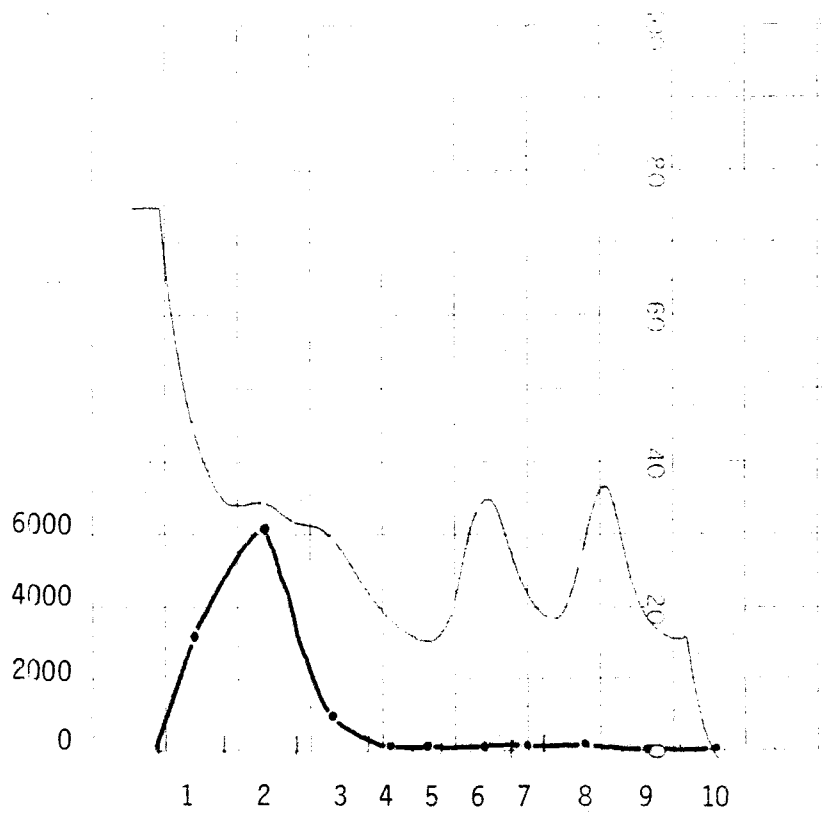


Figure 24. Lack of binding of T4 dCMP hydroxymethylase to purified *E. coli* rRNA. Conditions are the same as Fig. 16. Activity is in CPM of tritium released from the 5 position of dCMP per 100 μ l of sucrose gradient fraction per hour of incubation. Upper line denotes A₂₈₀₋₃₁₀.

host proteins were specifically retained by this gene 32 protein column. Nine of the T4 proteins were identified as being involved in either DNA replication or genetic recombination. They now use the column on a preparative scale for purification of the bound proteins. For our purposes purified dCMP hydroxymethylase was bound to an Affi-Gel matrix as described in Methods and by Formosa et al (1983). In addition, Gerry Lasser prepared separately a T4 dihydrofolate reductase and a host nucleoside diphosphokinase protein Affi-Gel column. ¹⁴C labeled phage early proteins were prepared as described in Materials and Methods. I prepared two control columns by binding bovine serum albumin to one column and ethanolamine to another. 5,000,000 cpm of labeled protein (500 μ l) was added to each column, which was then washed with buffer containing 50 mM KCl. Adsorbed protein was eluted with 200 mM and 600 mM KCl washes, sequentially. The results are plotted in Figures 25-29. Note that the two phage proteins, dihydrofolate reductase and dCMP hydroxymethylase, seem to be relatively inert since they adsorbed far less protein than did the host enzyme nucleoside diphosphate kinase or the two controls, bovine serum albumin and ethanolamine. These experiments suggest that, under conditions where the Alberts laboratory demonstrated positive protein-protein interactions (well above control values), the dNTP-synthesizing enzymes assayed show relatively little protein-protein interaction with other early T4 phage

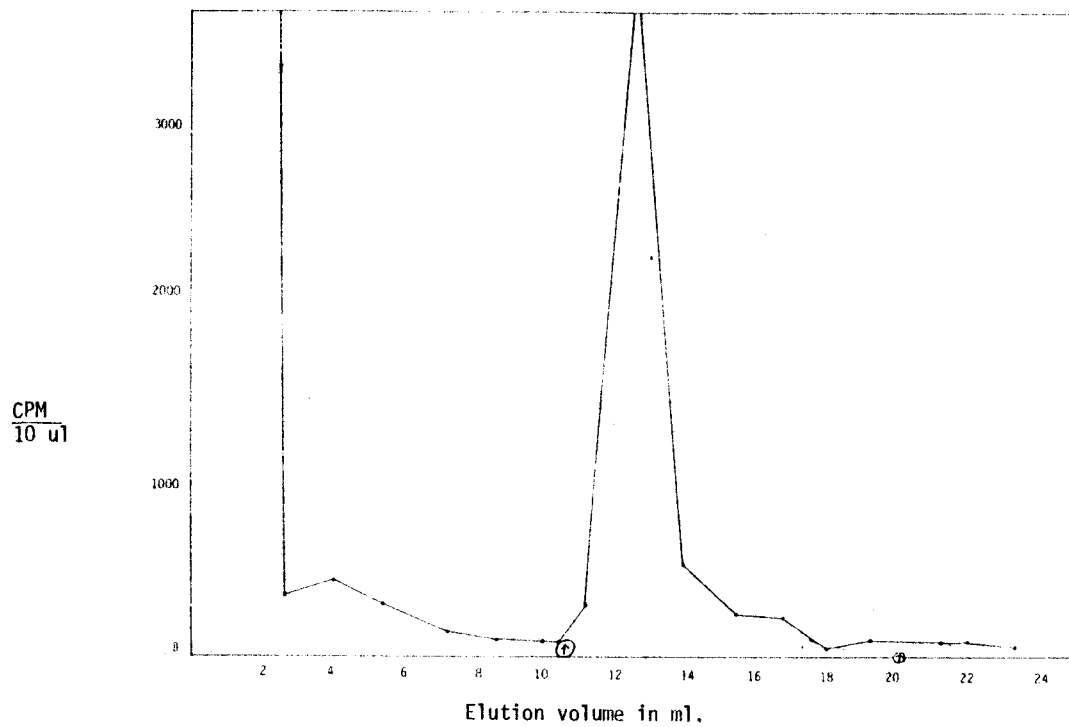


Figure 25. Elution profile from an ethanolamine coupled Affi-Gel control column. The activated column was saturated with ethanolamine. Arrows indicate the points of buffer change to 0.2 M and 0.6 M KCl, respectively.

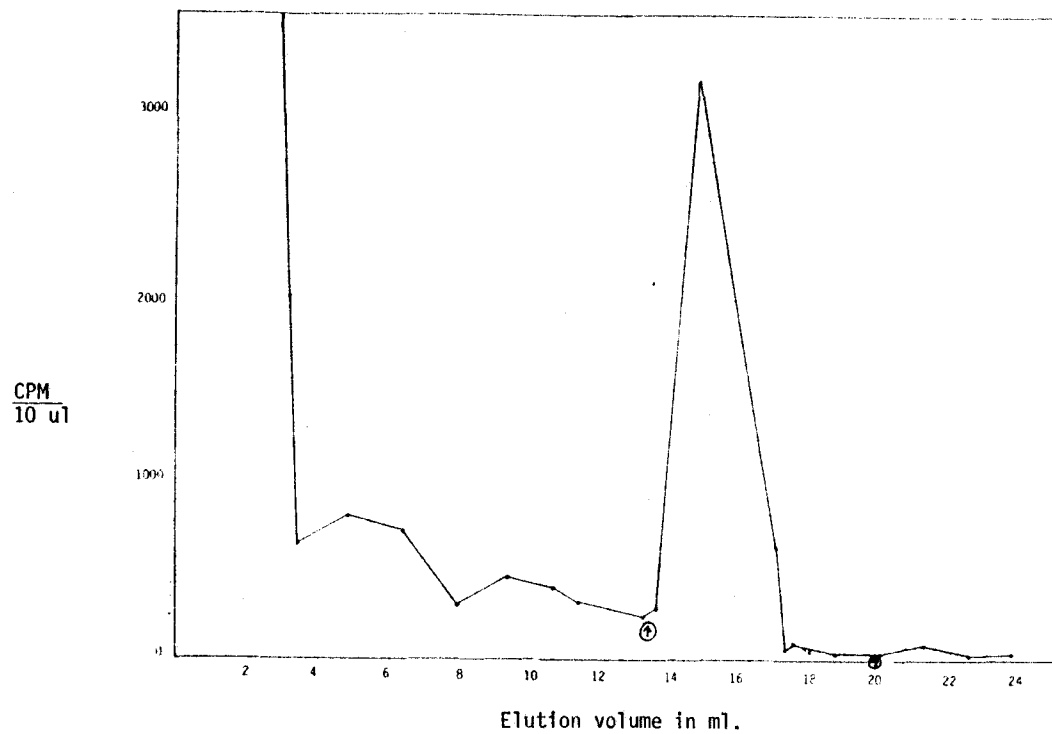


Figure 26. Elution profile from a bovine serum albumin coupled Affi-Gel control column. 5 mg of protein was bound to the column. Arrows indicate the points of buffer change to 0.2 M and 0.6 M KCl, respectively.

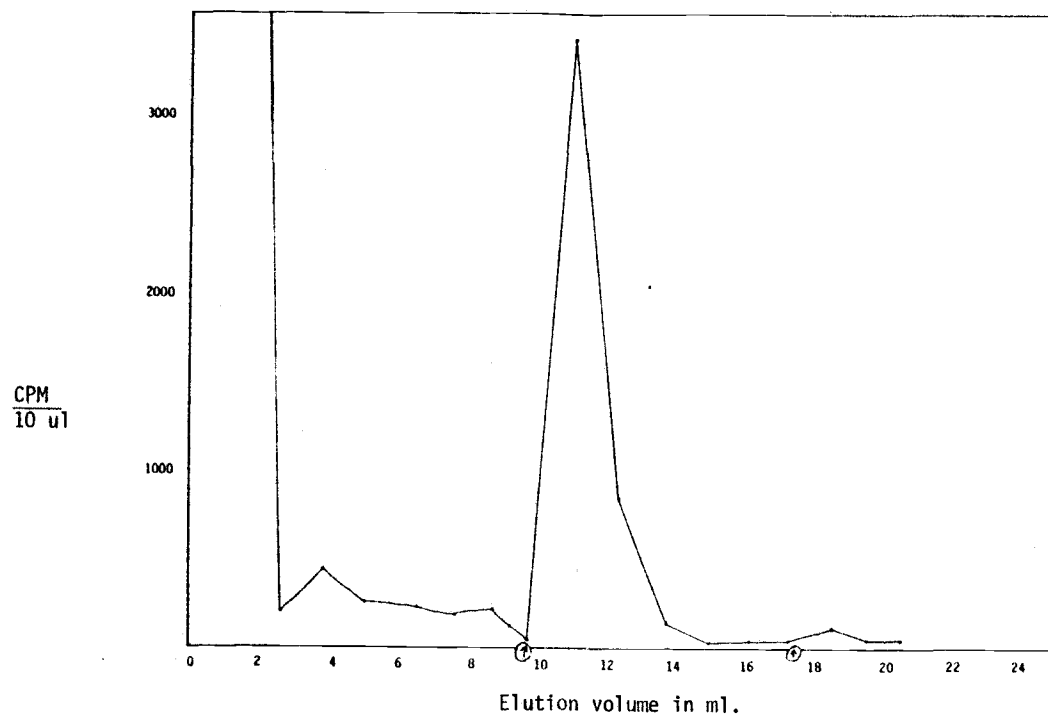


Figure 27. Elution profile from an *E. coli* nucleoside diphosphate kinase bound Affi-Gel column. 1 mg of protein was bound to the column. Arrows indicate the points of buffer change to 0.2 and 0.6 M KCl, respectively.

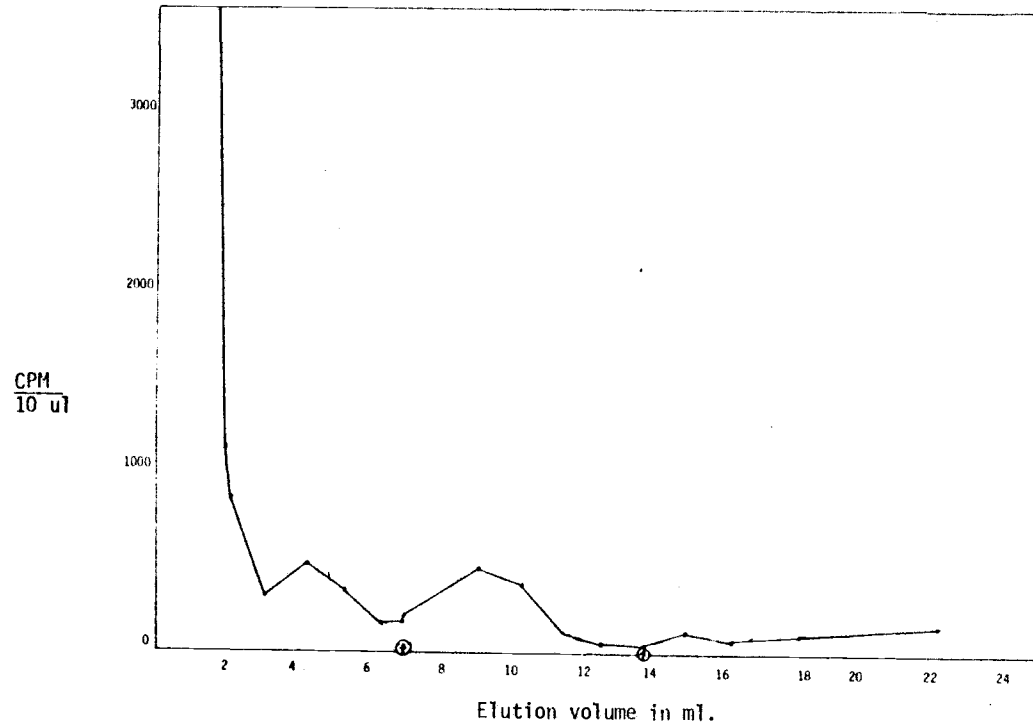


Figure 28. Elution profile from a T4 phage dihydrofolate reductase coupled Affi-Gel column. 4.8 mg of protein was bound to the column. Arrows indicate the points of buffer change to 0.2 M and 0.6 M KCl, respectively.

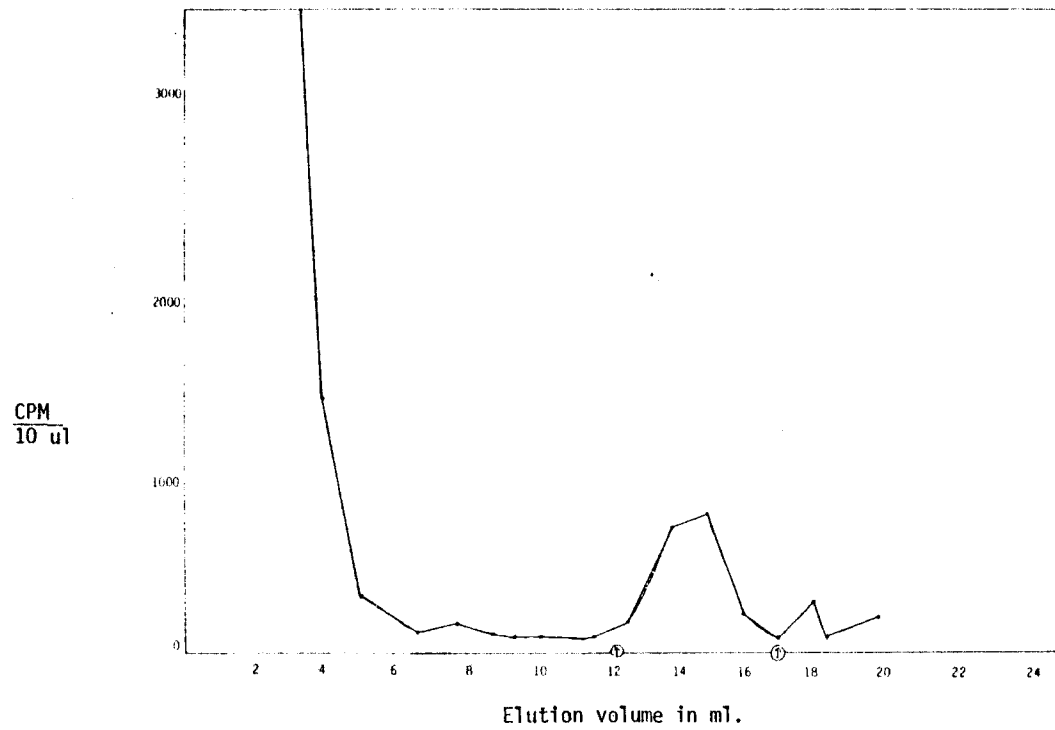


Figure 29. Elution profile from a phage dCMP hydroxymethylase coupled Affi-Gel column. 1.5 mg of protein was bound to the column. Arrows indicate the points of buffer change to 0.2 and 0.6 M KCl, respectively.

proteins. Final conclusions await the development of fluorograms of polyacrylamide gels used to detect whether binding is general or specific in nature.

PART 3: Observations Regarding Kinetically Coupled Activity

Effect of Mg⁺⁺ Ion on Kinetically Coupled Activity

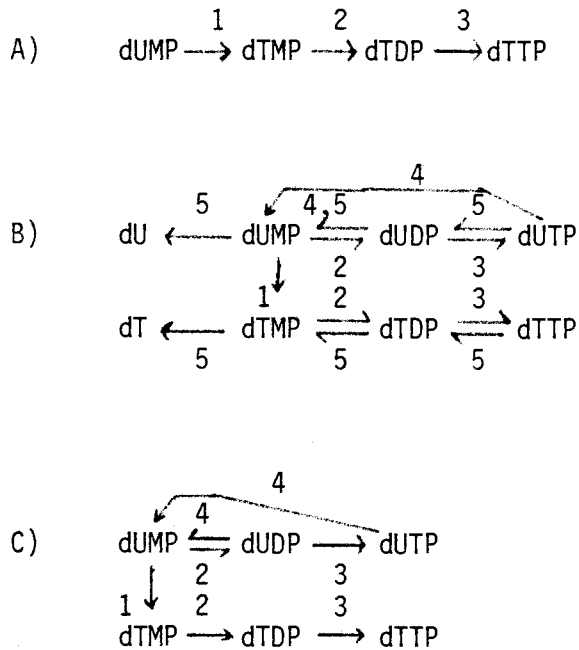
The sedimentation data presented above show that aggregation of dNTP-synthesizing enzymes is not correlated with DNA synthesis. I, therefore, decided to reexamine some of the other lines of evidence favoring the hypothesis of a specific enzyme complex to see if other explanations were possible. To support the idea that a rapidly sedimenting aggregate of dNTP-synthesizing enzymes is an organized complex rather than a non-specific aggregate, this laboratory has studied the kinetics of multistep reactions involving enzymes of the proposed complex (Reddy et al 1977; Allen et al 1983). The first, and by far the most extensively studied, involves the formation of dTTP using dUMP as the initial substrate. This three step reaction sequence reached its maximal rate within a few seconds when catalyzed by enzymes of the aggregate (Fig. 8). The authors (above) stated that 'an equivalent mixture of uncomplexed enzymes required nearly 20 minutes before dTTP synthesis reached its maximal rate'. It was concluded that the effect of the aggregate was to decrease the volume in which the intermediates are free to diffuse.

During my review of this material about the coupled assay I made several observations which have led to an alternative explanation for the observed experimental

results. The first involves the presence of Mg^{++} ion during the course of these assays. All of the sucrose gradient fractions assayed for coupled activity were first dialyzed in a 5 mM Mg^{++} -containing buffer for the purpose of removing the sucrose, which interferes with the spotting of samples on thin layer chromatography plates (Reddy et al 1977). Unpublished results from that same time period show 5 mM magnesium to reduce aggregation from between 70% to 100%. The existence of coupled activity in the presence of Mg^{++} ion directly contradicts the effect seen with Mg^{++} on rapid sedimentation. The 5 mM Mg^{++} is in addition to the 25 mM Mg^{++} that is contained in the buffer used to assay each of the individual enzymes and coupled activity. Centrifugation analysis indicates that the enzymes exist as monomers under such high magnesium assay conditions.

The Existence of Additional Pathways

If the enzymes do exist as monomers during the course of the assay then why does a small initial lag time exist when using the rapidly sedimenting fraction while a much slower rate and longer lag time is seen with the slowly sedimenting fraction π This question can be answered if one views the reaction sequence as being much more complex than was originally suggested by the authors. Figure 30a shows the reaction sequence as originally proposed by the authors. However, Allen et al 1983 demonstrated that, in addition the expected dTTP, dUTP was present and made up



1 = Thymidylate Synthase

2 = Nucleoside Monophosphate Kinase

3 = Nucleoside Diphosphate Kinase

4 = dUTPase-dCTPase

5 = 5' Nucleotidase

Figure 30 A,B,C. Proposed pathways for in vitro kinetically coupled enzyme assay. A, Pathway as originally proposed (Reddy et al. 1977). B, Pathways as catalyzed by enzymes at the top of the gradient. C, Pathways catalyzed by enzymes at the bottom of the gradient.

half of the total product measured. This activity is due to the phage enzyme deoxyribonucleotide monophosphokinase and the host diphosphokinase, which phosphorylate the deoxyuridine nucleotides as well as the deoxythymidine nucleotides (Bessman). This additional contribution to product was not taken into account in the computer simulation that was performed to simulate product formation by uncomplexed monomer enzymes. The unexpected contribution by dUTP can partially account for the smaller lag time and greater output.

However, this extra pathway does not explain why, in all of the various coupled assays performed, less product accumulates from fractions taken from the top of the gradient even though these often contain greater quantities of enzyme activities when measured individually. I have found this lack of product formation, when using enzymes from the top of the gradient, is due to an uneven distribution along the length of the gradient of the host enzyme 5' nucleotidase. Figure 31 shows the results of a ^{32}P release assay for measuring the activity of the constitutive host enzyme, using ATP as substrate. 5' nucleotidase specific activity for dUMP in a crude extract is four fold greater than that of thymidylate synthase (Neu 1967). Such an activity readily explains why such a large difference exists in the formation of product between the top and bottom gradient fractions. My revisions of the enzyme activity pathways for the top and bottom

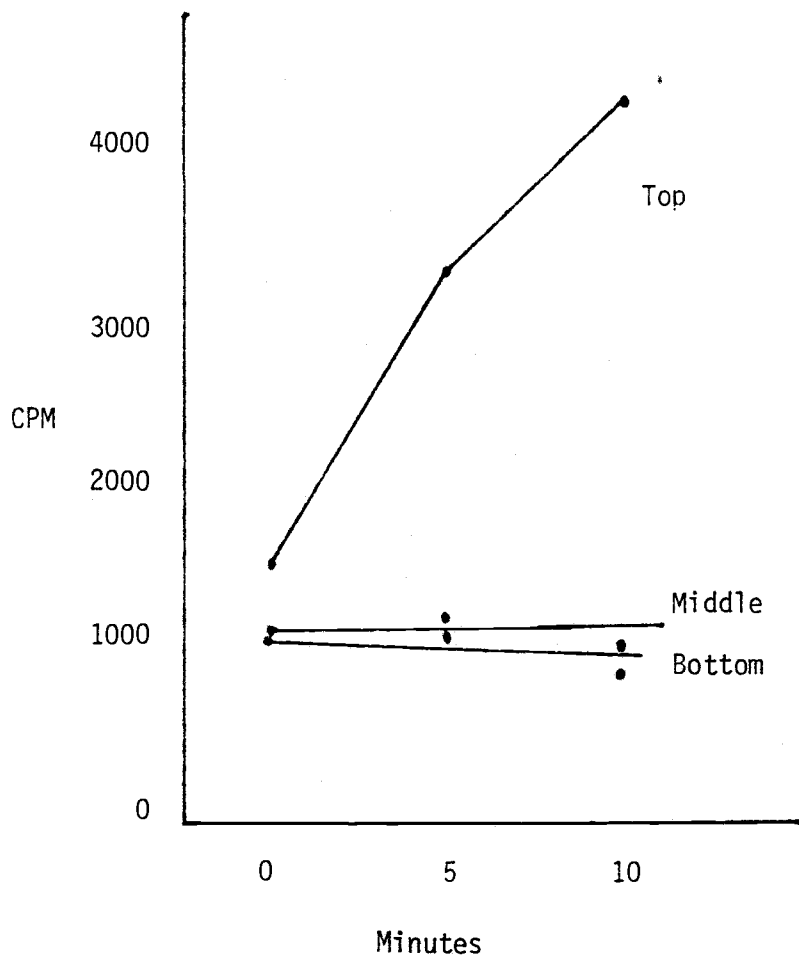


Figure 31. 5' nucleotidase assays of the top, middle, and bottom fractions of a sucrose gradient separation of an extract of T4 infected *E. coli*. (Assayed using release of gamma P^{32} ATP.)

fractions of the gradient are outlined in Fig. 30b,c.

Non-reproducibility of Initial Results

Another likely reason for the lack of correlation between the computer simulation and the results seen, when using enzyme from the bottom fraction, is that the enzyme values used in the simulation do not agree with all other values obtained during that same time period, as shown in Table 3. Since all of the previous values are fairly reproducible, and agree with my recently obtained data, the possibility that some experimental error was performed during that particular assay seems probable, especially since the same assay buffer is used for both kinase enzymes. These kinase enzyme activities deviate while thymidylate synthase (for which a separate assay buffer is used) is in accordance with previous values.

Underestimation of the real kinase activities would produce a computer simulated profile with a longer lag period and lower rate of activity as compared with the observed activity.

Consensus Value Computer Simulation

To test the possibility that the nucleotide kinase enzyme activities were underestimated in the published computer simulation of coupled activity, Gerry Lasser and I wrote a program to simulate nucleotide concentrations using the same kinetic assumptions as Reddy et al . 1977. Figure

<u>Figure</u>	<u>Enzyme Assayed</u>		
	<u>T.S.</u>	<u>M.P.K.</u>	<u>D.P.K.</u>
<u>PNAS 1977</u>			
2	1.3	150	400
3A	---	220	1000
3B	---	230	900
<u>Thesis (Reddy)</u>			
7A	2.8	160	---
7B	---	170	800
<u>Thesis (Weitz)</u>	1.0	295	1250
<u>Computer Simulation</u>	2.0	25	100

Table 3 . Enzyme activities from rapidly sedimenting fraction of 5-20% sucrose gradients. Note the lack of correlation between values of M.P.K. and D.P.K. used in the computer simulation with the other values above. Units are in nmoles/min./ml.

32 is a version of the program with Vmax values that correspond to the consensus values for the two nucleotide kinase enzymes. The results are tabulated in Table 4A and graphically represented in Figure 33. This simulation suggests that the experimental data can be fit with the assumption that all of the enzymes are uncomplexed. Nucleotide kinase values as stated by Reddy et al . were used as a control and our results, listed in Table 4B, agree fairly well with their earlier simulation.

```

PROGRAM COMP
C
C THIS PROGRAM CALCULATES THE VALUE OF DUMP AT 1 SEC INTERVALS
C AND PRINTS IT AT 1 MIN INTERVALS
C DUMP,DTMP,DTDP,DTTP ARE THE CONCENTRATIONS OF SUBSTRATES.
C
C DDUMP,ETC. IS THE CHANGE IN CONCENTRATION/SEC
C
C MPKF,DPKF ARE THE RESPECTIVE FORWARD RATES.
C
INTEGER X,N
REAL DUMP,DDUMP,DTMP,DDTMP,DTTP,DTDP,DDTDP,DDTTP,MPKF,DPKF
DDUMP = 0.
DUMP = 100.
DTMP = 0.
DDTMP = 0.
DTDP = 0.
DTTP = 0.
DDTDP = 0.
DDTTP = 0.
X=1
PRINT*, '      MIN      DUMP      DTMP      DTDP
1DTTP'
DO 100 I = 1,900
DDUMP = .025*(DUMP)/(20+DUMP)
DUMP = DUMP - DDUMP
MPKF = 2.*(DTMP)/(120 + DTMP)
DDTMP = DDUMP-MPKF
DTMP = DTMP + DDTMP
DPKF = 9.*(DTDP)/(200. + DTDP)
DDTDP = MPKF - DPKF
DTDP = DTDP+DDTDP
DTTP = DTTP + DPKF
X = X + 1
IF (X .NE. 60) GO TO 100
X = 1
N=N+1
PRINT*,N,DUMP,DTMP,DTDP,DTTP
100 CONTINUE
REWIND 6
CLOSE (UNIT=5)
STOP
END

```

INSET	
$\frac{d(dUMP)}{dt} = -\frac{V_{max}^{TS} [dUMP]}{K_m^{TS} + [dUMP]}$	
$\frac{d(dTMP)}{dt} = \frac{V_{max}^{TS} [dUMP]}{K_m^{TS} + [dUMP]} - \frac{V_{max}^{dNMPK} [dTMP]}{K_m^{dNMPK} + [dTMP]}$	
$\frac{d(dTDP)}{dt} = \frac{V_{max}^{dNMPK} [dTMP]}{K_m^{dNMPK} + [dTMP]} - \frac{V_{max}^{NDPK} [dTDP]}{K_m^{NDPK} + [dTDP]}$	
$\frac{d(dTTP)}{dt} = \frac{V_{max}^{NDPK} [dTDP]}{K_m^{NDPK} + [dTDP]}$	

Figure 32. Program used to generate concentrations of nucleotides as a function of time for the coupled assay shown in figure 29A. The steady state equations used to generate the program are shown in the inset. Enzymes are assumed to be uncomplexed.

A)

MIN	DUMP	DTMP	DTDP	DTTP
1	98.77208	0.7869647	0.2072636	0.2336933
2	97.54672	1.080663	0.3611804	1.011435
3	96.32397	1.189823	0.4234949	2.062699
4	95.10389	1.229297	0.4467263	3.219920
5	93.88653	1.242621	0.4548993	4.415950
6	92.67193	1.245842	0.4573477	5.624885
7	91.46014	1.245240	0.4576156	6.837003
8	90.25124	1.243153	0.4570453	8.048568
9	89.04528	1.240473	0.4561444	9.258127
10	87.84229	1.237527	0.4551049	10.46510
11	86.64235	1.234443	0.4539990	11.66924
12	85.44552	1.231268	0.4528539	12.87040
13	84.25185	1.228017	0.4516792	14.06849
14	83.06142	1.224697	0.4504784	15.26344
15	81.87428	1.221307	0.4492523	16.45518

B)

MIN	DUMP	DTMP	DTDP	DTTP
1	98.77208	1.156461	6.4990006E-02	6.4708949E-3
2	97.54672	2.177948	0.2275749	4.7755711E-2
3	96.32397	3.081729	0.4477031	0.1465883
4	95.10389	3.882450	0.6979907	0.3156618
5	93.88653	4.592512	0.9599964	0.5608609
6	92.67193	5.222960	1.221556	0.8835559
7	91.46014	5.782768	1.474887	1.282201
8	90.25124	6.280090	1.715235	1.753442
9	89.04528	6.721935	1.939934	2.292879
10	87.84229	7.114439	2.147726	2.895576
11	86.64235	7.462977	2.338297	3.556412
12	85.44552	7.772284	2.511949	4.270291
13	84.25185	8.046530	2.669361	5.032298
14	83.06142	8.289402	2.811445	5.837771
15	81.87428	8.504167	2.939229	6.682352

Table 4 A,B. The tables present the various nucleotide concentrations at one minute intervals. Enzymes are assumed to be present at consensus levels. A. Enzymes are assumed to be present at levels reported by Reddy *et al.*, 1977, table B.

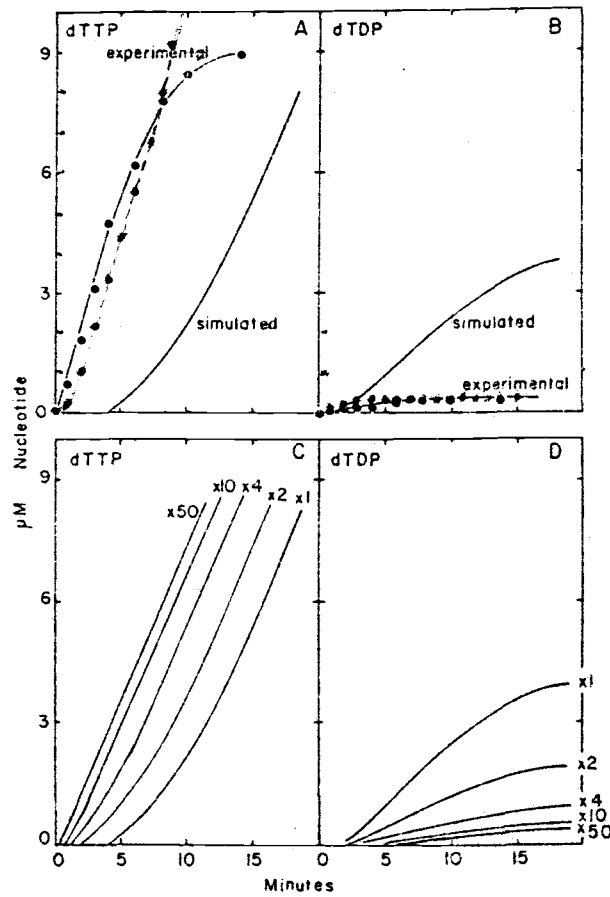


Figure 33. This reproduction of Figure 8 has been modified to include dTTP and dTDP concentrations from Table 4 A. Enzymes are assumed to be present at consensus levels rather than at the levels used in the simulation by Reddy *et al.*, shown above and in Figure 8.

PART 4: Compartmentation of Nucleotides In Situ

Verification of 5' nucleotidase activity in T4 infected E.coli

In light of the sedimentation and coupled activity data presented above I decided to review the in situ evidence for nucleotide compartmentation. The suggested functional compartmentation of DNA precursors is based primarily on the finding that sucrose plasmolysed T4-infected cells incorporate dNMP's into DNA more rapidly than the corresponding dNTP's, even though the dNTP's are the proximal DNA precursors in vivo, as shown in Fig. 7. Evidence also suggested that dNTP's in this in situ system were dephosphorylated before their ultimate incorporation into DNA (Reddy and Mathews, 1978). The authors hypothesized that the dNTP-synthesizing enzyme complex restricts access of dNTP's to DNA polymerase at the site of replication and that the complex preferentially accepts dNMP's over dNTP's and delivers the twice phosphorylated precursors to the site of replication. However, breakdown of dNTP's to dNMP's by a nucleotidase before gaining access to DNA polymerase directly, rather than via complex, seemed to me a possible alternative. Figure 34 is a profile of dTTP nucleotidase activity from a crude extract of T4 infected cells. I chose dTTP because dTMP and dTTP were the labeled nucleotides used by Reddy and Mathews. Subsequently I was shown an article on the constitutive periplasmic

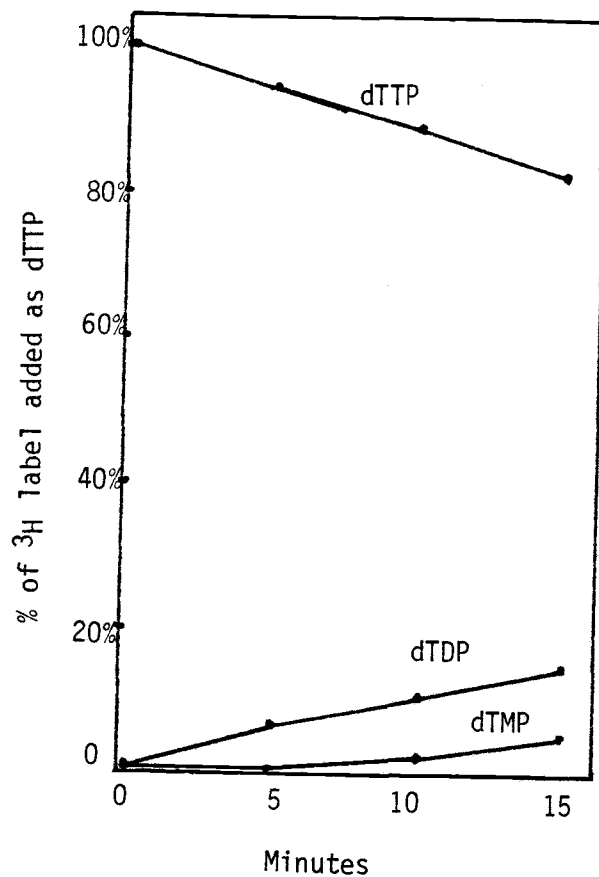


Figure 34. Assay of 5' nucleotidase activity in crude extract of T4 infected *E. coli*. The reaction conditions and chromatography were the same as for the coupled activity experiments of Reddy *et al.* 1977. 5' nucleotidase removes the terminal phosphate from any 5' nucleotide (Neu, 1967).

enzyme 5'nucleotidase from E.coli . My activity was found to be equal to that quoted for an extract from an uninfected host (Neu 1967). Therefore, no increase or decrease in nucleotidase activity is seen upon infection with T4. Osmotic shock, such as sucrose plasmolysis, is used to release this and other periplasmic proteins. This enzyme, therefore, accounts for the nucleotide dephosphorylation seen by Reddy and Mathews.

Membrane vs enzyme complex compartmentation

Recently, another laboratory looked at incorporation of thymine precursors into DNA in T4 infected cells. Melamed and Wallace (1983) presented evidence that sucrose plasmolysed cells incorporate nucleosides into DNA more rapidly than are the phosphorylated nucleosides, Figure 35. The rate of incorporation is inversely related to the level of phosphorylation (i.e., from greatest to least: TdR, dTMP, dTTP). Surprisingly, this same general phenomenon was also seen with intact non-plasmolysed cells. Plasmolysis seemed to have little effect on which DNA precursor was preferentially incorporated. These results, taken together, indicate to me that preferential incorporation of dNMP's over dNTP's into DNA is due to the kinetics of nucleotide dephosphorylation. Once the nucleotide is converted to the non-phosphorylated nucleoside it can pass through the largely intact membrane via nucleoside active transport at which point it becomes available to cytoplasmic enzymes

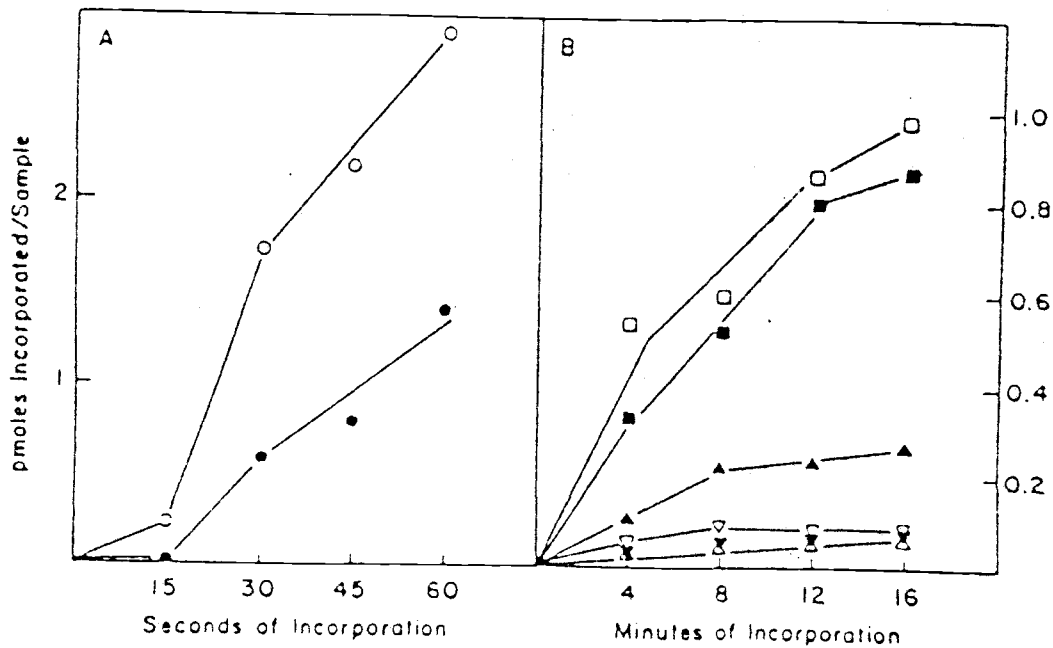


Fig. 35 DNA synthesis in plasmolysed and non plasmolysed wild-type T4-infected cells. Synthesis was measured by the incorporation of (A) $1 \mu\text{M}$ ^3H TdR, (B) $1 \mu\text{M}$ ^3H thymine, $1 \mu\text{M}$ ^3H dTMP or $1 \mu\text{M}$ ^3H dTTP into acid precipitable material. Infected cells were pelleted 15 min after infection at 37°C and resuspended 100 fold concentrated in either M9 medium or plasmolysis solution. $5 \mu\text{l}$ of cell suspension was diluted 6-fold into the indicated precursor containing reaction mix. $5 \mu\text{l}$ samples were spotted onto Whatman GFA filters, TCA precipitated and counted as described in the Materials and Methods. Symbols: Unfilled, nonplasmolysed: ▽ thymine, ○ TdR, □ dTMP, △ dTTP. Filled, plasmolysed: ▼ thymine, ● TdR, ■ dTMP, ▲ dTTP. Adapted from Melamed and Wallace, 1983.

such as nucleotide kinases and DNA polymerase.

The possibility existed that the study of DNA precursor uptake by Melamede and Wallace was not valid for comparison with the results of Reddy and Mathews (1978). This objection was based on the fact that Reddy and Mathews used 83 μM of each of the DNA precursors in their reaction mixture while the other group used 1 μM . It was thought that a lower concentration of labeled precursor could be more easily diluted by endogenous cellular pools. To explore this possibility I repeated some of Melamede and Wallaces' work using the conditions of Reddy and Mathews. Figure 36 shows that sucrose permeabilization had little effect on DNA precursor incorporation. This evidence suggests that cellular membranes are relatively intact and that little permeabilization has occurred. Thus, membrane transport of nucleosides across the membrane can account for the preferential incorporation of distal precursors in sucrose plasmolyzed cells, as is known to occur in normal cells.

Lack of correlation with other permeabilization methods

In T4-infected cells made permeable to nucleotides by treatment with toluene, dNTP's are preferentially incorporated at a rate ten fold over that of 3 dNMP's and one dNTP (Dicou and Cozzarelli, 1973). This type of permeabilization maintains features of the in vivo process. Synthesis is specific for T4 phage, requires

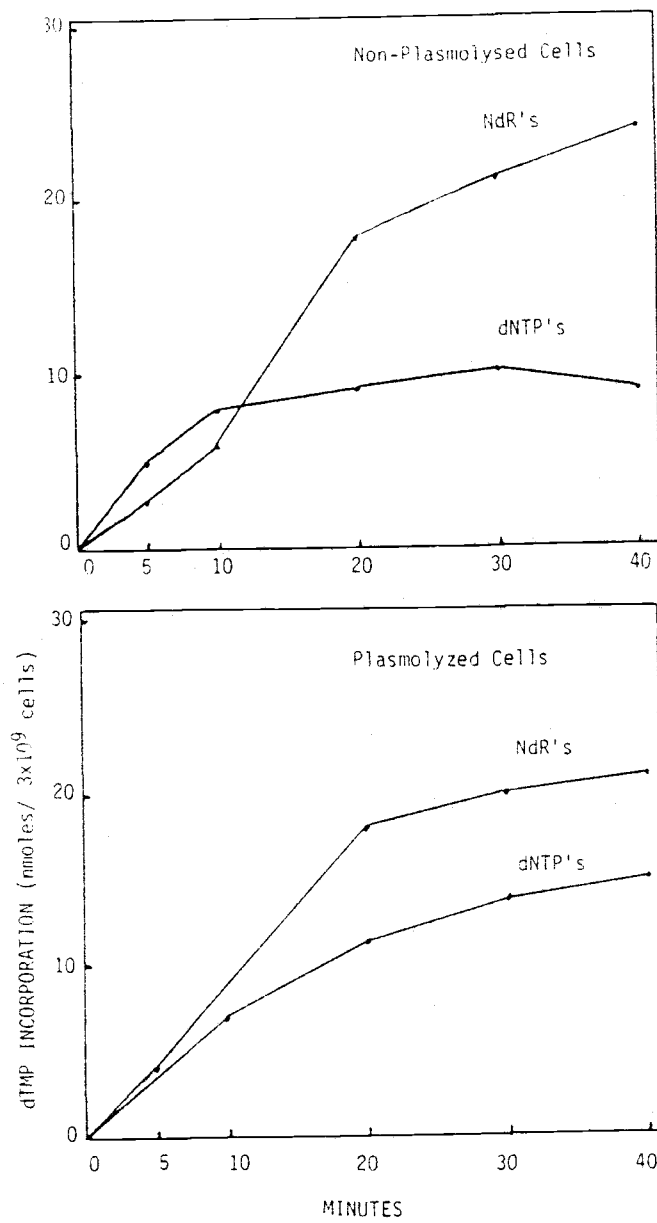


Figure 36. Effects of plasmolysis upon T40-directed DNA synthesis *in situ*. Experimental conditions were as described by Reddy and Mathews, 1978.

deoxyribonucleoside triphosphates and Mg^{++} , and is absent after infection by T4 mutants unable to synthesize DNA in vivo .

In cellophane disc gentle lysates of T4 infected cells the four dNTP's are incorporated into DNA at a rate four fold over that of the four dNMP's (Huang, 1983). This system involves a gentle and complete lysis of infected cells on the surface of semipermeable cellophane disks. The system retains all of the known features of the T4 infected in vivo process. The advantage of this system lies in the ability to carry out in vitro protein complementation experiments. This method is based on that first used by Schaller et al (1972) to study E. coli replication. Both of these alternative permeabilization methods suggest that dNTP's are the preferred precursors for DNA synthesis in situ .

IV. DISCUSSION

PART 1: Enzyme Aggregation and Rapid Sedimentation

T4 thymidylate synthase binds nucleic acid

Initially, this laboratory and, more recently, others (Reddy and Pardee, 1980; Rao and Kisliuk, 1983) have reported the existence of rapidly sedimenting thymidylate synthase in crude cell extracts. They have suggested that this is a characteristic of a functionally meaningful aggregate of DNA precursor synthesizing enzymes. My results show that rapid sedimentation of T4 thymidylate synthase is not observed when either one or both of its two enzyme cofactors are present. Evidence suggests that the enzyme binds to ribosomal subunits due to an affinity for single-stranded nucleic acid. This unexpected affinity, present even in the absence of other T4 proteins, can be explained as a consequence of the enzyme being part of the morphological structure of the virus particle. As presented in the introduction, evidence exists and Kozloff has proposed that the enzyme binds the polyglutamate portion of the fohylhexaglutamate found in the phage baseplate. As part of a morphological structure requiring increased stability, one might expect that the T4 enzyme would have a greater affinity for fohylpolyglutamates than thymidylate synthases from other species. The unexpected ability of the T4 enzyme to bind single-stranded nucleic acid may be a

manifestation of its morphological role since polyglutamate and single-stranded nucleic acid are both linear polyanionic structures. In accord with this idea, Maley et al (1979) found that the T2 enzyme binds pteroylhexaglutamate two orders of magnitude more tightly in the absence of Mg^{++} than in its presence. In contrast, the E. coli enzyme binds more tightly when Mg^{++} is present. Note that both nucleic acid and polyglutamate binding by T4 thymidylate synthase are Mg^{++} sensitive. As might be predicted by this model, a pteridine ring analog which lacks a polyglutamate tail, such as methotrexate, did not show this differential selectivity. Using data presented by Kisliuk (1981), Dr. Mathews put together the data shown in Figure 37. This graph compares the effectiveness of pteroylglutamate as an inhibitor of various thymidylate synthases as a function of the number of glutamate residues. The values obtained by Maley et al (1979), mentioned previously, are superimposed for the purpose of comparison. As can be seen, the phage enzyme and the L. casei enzyme are clearly separated from the others. Please note that inhibition is presented on a log scale. Due to the similarity between the phage and L. casei enzymes one might ask why the bacterial enzyme didn't also bind nucleic acid. I can suggest two possible explanations. First, all of the values reported by Kisliuk are in the presence of Mg^{++} . The Maleys' data show that removal of Mg^{++} causes an increased affinity for the inhibitor when

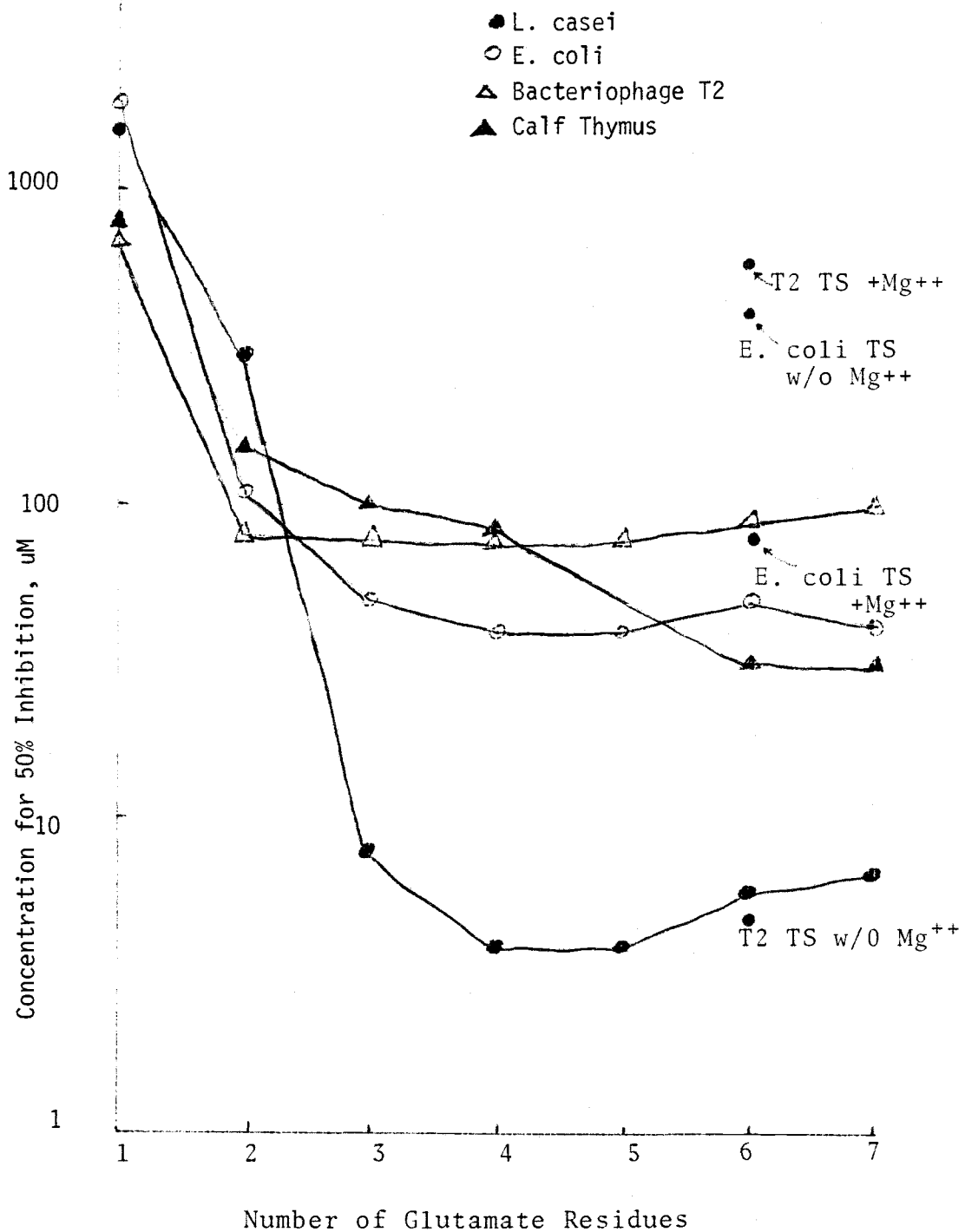


Figure 37. Inhibition of various thymidylate synthases by pteroylpolyglutamate as a function of the number of glutamate residues. Data from Kisliuk (1981) and Maley et al. (1979).

the E. coli enzyme is used. An analogous behavior by the L. casei enzyme would greatly reduce its binding affinity and leave the phage enzyme alone in terms of its binding affinity under low Mg^{++} conditions. A second, and more speculative, explanation is based on the pI of the phage thymidylate synthase. All of the purified dNTP synthesizing enzyme pI's determined to date in our laboratory fall into a pH range of 4.5 to 5.5. Additionally, thymidylate synthase from L. casei and E. coli also fall into this same range. The T4 enzyme with a pI of 7.2 may be expected to have a rather marginal solubility under physiological conditions of pH. The enzyme partially precipitates from solution if the purification process is performed with a buffer pH around 7 (personal observation; personal communication Gladys Maley). This unusual behavior may actually be advantageous for a protein that must become part of the phage baseplate. A low solubility would reduce the free energy needed for the enzyme to leave the aqueous phase and to condense on to the base plate. This nonspecific partial reduction of the free energy of binding is somewhat analogous (in function but not mechanism) to the entropic binding of site specific DNA binding proteins. However, I have not seen this suggested before as a general mechanism in morphogenesis.

Nature of Protein-Protein Interactions

Clearly the properties of T4 thymidylate synthase

differ from those of many other dNTP synthesizing enzymes. Therefore, knowledge about its mechanism of aggregation reveals little about the properties of the other dNTP synthesizing enzymes. Ever since their observation that RNAse and DNase treatments had no effect on the rapid sedimentation of dNTP synthesizing enzymes (Reddy etal 1977), the authors have suggested that protein-protein interactions are involved in maintaining the integrity of the putative complex. This observation at first seems to contradict the notion that T4 thymidylate synthase binds to ribosomes via an affinity for rRNA. However, ribosomes are known to be resistant to RNAase treatment. Also, an RNAse might not have access to rRNA that is protected by tightly bound thymidylate synthase or other bound cytoplasmic proteins.

At this point I shall review the general forces known to stabilize noncovalent assemblies of protein subunits. The forces known, experimentally, to destabilize rapid sedimentation of the dNTP-synthesizing enzymes will be compared with these protein-protein interactions. Table 5 presents a breakdown of the known types of contacts found at the subunit interfaces of some widely divergent proteins. A tight steric fit between subunits is suggested by the overwhelming number of Van der Waals contacts seen. Note that ionic forces play a rather limited role in stabilizing these subunit interactions. An analysis of the energy required for subunit-subunit stability suggests that

Nature of subunit interfaces

Protein	Symmetry	Regions in contact	Van der Waals contacts	Hydrogen bonds	Ion pairs
α -Chymotrypsin	C_2	A	443	9	1
		B	57	6	—
Concanavalin A	D_2	to A	—	2	—
		to B	142	14	6
		to C	174	14	—
Hemoglobin Oxyhemoglobin	C_2	$\alpha_1\beta_1$	110	5	—
		$\alpha_1\beta_2$	80	1	—
		$\alpha_1\alpha_2$	—	—	—
		$\beta_1\beta_2$	—	—	—
Deoxyhemoglobin	C_2	$\alpha_1\beta_1$	98	5	—
		$\alpha_1\beta_2$	69	1	1
		$\alpha_1\alpha_2$	—	—	2
Insulin	D_3	$\beta_1\beta_2$	—	—	1
		OP	111	8	—
		OQ	99	2	1

SOURCE: Adapted from A. Liljas and M. Rossman, *Ann. Rev. Biochem.* 43:485 (1974).

Table 5. Forces that stabilize protein-protein subunit interactions.

the interactions required to bring two subunits together must be on the order of -30 to -50 kcal/mole (Cantor and Schimmel, 1980). A further analysis shows that, although Van der Waals forces can provide a portion of the needed energy, the hydrophobic interaction (also due to the close fit) is responsible for the greatest energy contribution.

Experimentally, I have shown the rapid sedimentation of dNTP-synthesizing enzymes to be very sensitive to the divalent cation Mg^{++} and moderately sensitive to the monovalent cations Na^{+} and K^{+} . These results are in contrast to the present notion of the forces that stabilize protein-protein interactions. An appropriate model for comparison may be the 7 million dalton multisubunit protein pyruvate dehydrogenase complex. The complex requires Mg^{++} for catalysis, as does the proposed dNTP synthetic complex. However, unlike the proposed complex, the pyruvate dehydrogenase complex maintains its integrity in the presence of Mg^{++} or Ca^{++} . Such integrity in the presence of catalytically required cations seems to be an obvious and necessary feature of protein complex subunit interactions.

Behavior of Polyelectrolyte Macromolecules

Nucleic acids and proteins are polyelectrolyte macromolecules. Nucleic acids can be visualized as having a uniform negative charge density, while the sign and density of the charge can vary from one region to another on a protein. Proteins tend to have hydrophobic interiors and

hydrophilic surfaces. To reduce the potential magnitude of undesirable electrostatic interactions between macromolecules in a cell, where proteins are present at a concentration of around 200 mg/ml, the maintenance of a high counter ion level seems reasonable. Figure 38 illustrates typical ionic conditions found in a mammalian cell. Almost identical conditions are found in E.coli (Lusk et al 1968; Kao-Huang et al 1977).

Experimentally, researchers rarely use lysis buffers containing such high quantities of salt. Upon lysis, biological macromolecules are diluted into an environment with far less capacity to shield one polyelectrolyte from another. Additionally, entropically induced macromolecular condensations become very favorable in low ionic strength solutions. Such interactions are well documented in the case of operon repressor proteins and for ribosome purification. Many of the early methods of ribosome purification employed variants of that used by Tissieres et al (1959). This method involved lysis in dilute buffer, containing 10 mM MgCl₂, followed by repeated centrifugation in the same buffer. Even this concentration of salt didn't remove all of the extraneous proteins such as ribonuclease. Later techniques utilized salt 'washes' of 0.5 or 1 M NH₄Cl, which resulted in the removal of extraneous proteins without loss of ribosomal activity (Stanley et al 1966).

Nonspecific Ionic Interactions as Suggested Cause of Enzyme

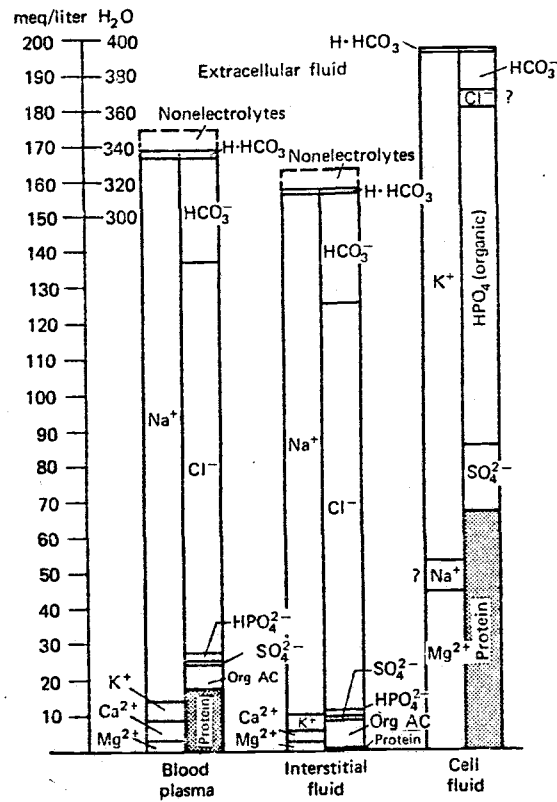


Figure 38.

Diagram showing major chemical constituents of three fluid compartments.

Height of left half of each column indicates total concentration of cations; that of right half, concentration of anions. Both are expressed in meq/liter of water. Note that chloride and sodium values in cell fluid are questioned. It is probable that, at least in muscle, the cytosol contains some sodium but no chloride.

Modified from Gamble. From Magnus I. Gregersen, in *Medical Physiology*, 11th ed., Philip Bard, ed., Mosby, St. Louis, MO. 1961, p. 307.

Aggregation.

Two parallels exist between the partial isolation of the proposed dNTP-synthesizing complex and that of ribosomes. The dNTP-synthesizing enzymes that rapidly sediment (not all T4 dNTP-synthesizing enzymes do) have always done so in very low salt buffers with sensitivity to even moderate levels of salt. Additionally, this aggregate of enzymes cosediments with ribosomal subunits. Aggregation is seen with or without T4 infection and is quantitatively independent of the number of DNA replication forks present in the cell. These observations are consistent with the idea that weak electrostatic interactions promote association of dNTP synthesizing enzymes (and other proteins) with the charged polyelectrolytes that make up the ribosomal subunits.

The ionic interactions responsible for enzyme aggregation may not be significant under the conditions of high ionic strength found in the cellular environment. Alternatively, it may be argued that the high protein concentrations found in the cell (200 mg/ml, Leninger) would favor greater protein-protein interaction, perhaps enough to stabilize the observed forces even in the presence of physiological salt concentrations. However, gel filtration studies show that of all the dNTP-synthesizing enzymes that can aggregate only a small amount of thymidylate synthase does at a protein concentration of around one mg/ml (personal communication, Joe Booth and Dan

Goldman of this laboratory). The protein concentration of the cell extracts used in my sedimentation experiments were around 20 mg/ml. Such a concentration was obtained by resuspending one volume of pelleted cells with three volumes of buffer before lysis. At this protein concentration enzyme aggregation is sensitive to physiological salt concentrations. Therefore, it seems reasonable to me that at a further ten fold increase in protein concentration, to match cellular levels, moderate salt concentrations would still interfere in vivo with the forces responsible for the observed aggregation in vitro .

PART 2: Concluding Summary

Investigators both here and in Dr. Greenberg's laboratory have been studying an aggregate containing enzymes of deoxyribonucleoside triphosphate biosynthesis in T4-phage infected bacteria. They suggest that it behaves as an organized complex, efficiently channeling DNA precursors to the replication apparatus. Dr. C. Friedman, in Protein-Protein Interactions, defines two criteria which must be met to prove the existence of a multi-enzyme complex: "Kinetic measurements must be coupled with independent measurements of protein-protein interactions by physical methods". According to this criterion, the results presented in this dissertation suggest that the proposed, T4 induced, dNTP-synthesizing enzyme complex, as studied in vitro and in situ, may have little basis in fact.

Previous publications have suggested that about 10 enzyme activities remain associated through several fractionation steps. This multi-enzyme aggregate has been reported to sediment through sucrose gradients at 15-20 S. Also, individual activities are kinetically coupled in crude preparations of this aggregate, such that in vitro it can initiate catalysis of multistep pathways with virtually no lag and with low accumulation of intermediates (Allen et al. 1983).

However, work presented here shows that aggregation of thymidylate synthase, the key enzyme of all kinetic

coupling studies, is not observed when either of its two enzyme cofactors, Mg^{++} or methylenetetrahydrofolate, is present. Evidence suggests that the enzyme binds to ribosomal subunits due to an affinity for single-stranded nucleic acids under conditions of low ionic strength. This unexpected affinity, present even in the absence of other T4 proteins, can be explained as a consequence of the enzyme being part of the morphological structure of the virus particle.

Nucleoside diphosphate kinase and adenylate kinase, two host enzymes of the proposed complex, are shown to sediment with the exact same pattern in uninfected cells. Thus, aggregation of these dNTP synthesizing enzymes is not influenced qualitatively or quantitatively by the increased number of DNA replication forks present in an infected cell. Sedimentation values presented here are 30-50 S irrespective of the number of enzyme activities present in the aggregate. This aggregation is sensitive to physiological concentrations of salt. Evidence suggests that aggregation is due to low salt-induced binding of cytoplasmic proteins to ribosomal subunits.

All enzyme mixtures previously assayed for kinetically coupled activity were first dialyzed in a magnesium-containing buffer which has been shown to partially or totally prevent aggregation. The assay buffer contains several times this amount of magnesium in addition to the methylenetetrahydrofolate mentioned above.

Experimental coupled activity can be simulated assuming that the enzymes are uncomplexed if one uses consensus enzyme concentrations.

Evidence of DNA precursor channeling in sucrose plasmolyzed, T4-infected cells is shown not to be consistent with other plasmolysis or gentle lysate systems. The discrepancy can be resolved by the demonstration that sucrose plasmolyzed, T4-infected cells may have relatively intact membranes.

The material presented here has not assessed the potential existence of a dNTP-synthesizing complex in vivo. At this time it seems difficult, experimentally, to rigorously explore such a concept. It is my hope that the work presented here will help to broaden the conceptual and experimental framework of future investigations in this field.

BIBLIOGRAPHY

- Allen, J.R., G.P.V. Reddy, G.W. Lasser, and C.K. Mathews (1980). *J. Biol. Chem.*, 225 , 7583-7588.
- Allen, J.R., J.W. Booth, D.A. Goldman, G.W. Lasser, and C.K. Mathews (1983). *J. Biol. Chem.*, 258 , 5746-5753.
- Belfort, M., Moelleken, A., Maley, G.F. and Maley, F. (1983) *J. Biol. Chem.* 258 , 2045-2051.
- Berglund, O. (1972) *J. Biol. Chem.* 247 , 7270-7281.
- Cantor, C.R., and Schimmel, P.R. (1980), p. 144-145, W.H. Freeman & Co., San Francisco.
- Capco, G.R., Krupp, J.R. and Mathews, C.K. (1973) *Arch. Biochem. Biophys.* 158 , 736-743.
- Chao, J., Leach, M. and Karam, J.D. (1977) *J. Virol.* 24 , 557-563.
- Chiu, C.S., and G.R. Greenberg. (1968). *Cold Spring Harbor Symp. Quant. Biol.*, 33 , 351-357.
- Chiu, C.S., K.S. Cook, and G.R. Greenberg, (1982). *J. Biol. Chem.*, 257 , 15087-15097.
- Chiu, C.S., Cook K.S. and Greenberg, G.R. (1983) *J. Biol. Chem.* 257 , 15087-15097.
- Chu, F., Maley, F., Maley, G.F. and Belfort, M. (1984) *Proc. Natl. Acad. Sci. USA*, in press.
- Cohen S.S., (1968). *Virus-induced enzymes*. Columbia University Press, New York.
- Dube, S.K. and Rudland, P.S. (1970) *Nature* 226 , 820-823.
- Dicou, L., and Cozzarelli, N. (1973) *J. Virology*, 12 , 1293-1302.
- Erikson, R.I., and W. Szybalski (1964). *Virology*, 22 , 111-120.
- Flanegan, J.B. and Greenberg, G.R. (1977) *J. Biol. Chem.* 252 , 3019-3027.
- Formosa, T., Burke, R.L., and Alberts, B.M. (1983) *Proc. Nat. Acad. Sci. USA*, 80 , 2442-2446.
- Fulton, A.B. (1982) *Cell* 30 , 345-347.

- Galivan, J., Maley, G.F. and Maley, F. (1974) *Biochemistry* 13 , 2282-2289.
- Huang, W.M., and Buchanan, J.M. (1974) *Proc. Nat. Acad. Sci. USA*, 71 , 2226-2230.
- Iwatsuki, N. (1977) *J. Biochem. (Tokyo)* 82 , 1347-1359.
- Johnson, J.R., Collins, G.M., Rementer, M.L., and Hall, D.H. (1976) *Antimicrob. Agents Chemother.* 9 , 292-300.
- Kao-Huang, Y., Revzin, A., Buttler, A.P., O'Connor, P., Noble, O., and von Hippel, P.H. (1977) *Proc. Nat. Acad. Sci. USA*, 74 , 4228-4232.
- Kisliuk, R.L. (1981) *Mol. and Cell. Biochem.* 39 , 331-345.
- Kikuchi, Y., and King, J. (1975) *J. Mol. Biol.* 99 , 645-672.
- Kozloff, L.M. (1983) in *Bacteriophage T4* (Mathews, C.K., Kutter, E.M., Mosig, G. and Berget, P.B., Eds.), p. 25-31. American Society for Microbiology, Washington, D.C.
- Lunn, C.A. and Pigiet, V. (1969) *J. Biol. Chem.* 254 , 5008-5014.
- Lusk, J.E., Williams, R.J.P., and Kennedy, E.P. (1968) *J. Biol. Chem.*, 243 , 2618-2624.
- Maley, G.F., Guarino, D.U., and Maley, F. (1967) *J. Biol. Chem.* 242 , 3517-3524.
- Maley, G.F., MacColl, R., and Maley, F. (1972) *J. Biol. Chem.* 247 , 940-945.
- Maley, G.F., Maley, F. and Baugh, C.M. (1979) *J. Biol. Chem.* 254 , 7485-7487.
- Maley, G.F., and Maley, F. (1982) *Biochemistry*, 21 , 3780-3785.
- Mathews, C.K., (1967) *J. Virol.* 1 , 963-967.
- Mathews C.K., (1971). *Bacteriophage Biochemistry*. Van Nostrand Reinhold Co., New York.
- Mathews, C.K. (1976) *Arch. Biochem. Biochem.* 172 , 178-187.
- Mathews C.K. (1977). *Compr. Virol.*, 7 , 179-294.

- Mathews, C.K. and J. Allen, (1983). in Bacteriophage T4 (Mathews, C.K., Kutter, E.M., Mosig, G. and Berget, P.B., Eds.), p. 59-70. American Society for Microbiology, Washington, D.C.
- Mathews, C.K. and Sinha, N.K. (1982) Proc. Natl. Acad. Sci. USA 79 302-306.
- Neu, H.C., (1967) J. Biol. Chem., 242 , 3896-3911.
- North, T.W., Stafford, M.E. and Mathews, C.K. (1976) J. Virol. 17 , 973-982.
- North, T.W., and Mathews, C.K. (1977) B. B. R. C. 77 , 898-904.
- Nossal, N.G., and Alberts, B.M. (1983) in Bacteriophage T4 (Mathews, C.K., Kutter, E.M., Mosig, G. and Berget, P.B., Eds.), p. 71-81. American Society for Microbiology, Washington, D.C.
- O'Farrell, P.Z., Gold, L.M., and Huang, W.M. (1973) J. Biol. Chem. 248 , 5499-5505.
- Plante, L., Gaumont, Y. and Kisliuk, R.L. (1978) Prep. Biochem. 8 , 91-98.
- Purohit, S., Bestwick, R.K., Lasser, G.W., Rogers, C.M., and Mathews, C.K. (1981) J. Biol. Chem. 256 , 9121-9125.
- Purohit, S. and Mathews, C.K. (1984) J. Biol. Chem., in press.
- Rao, K.N. and Kisliuk, R.L. (1983) Proc. Natl. Acad. Sci. USA 80 , 916-920.
- Reddy, G.P.V., and C.K. Mathews. (1978). J. Biol. Chem., 253 , 3461-3467.
- Reddy, G.P.V., A. Singh, M.E. Stafford, and C.K. Mathews. (1977). Proc. Nat. Acad. Sci. USA, 74 , 3152-3156.
- Reddy, G.P.V., and A.B. Pardee. (1980). Proc. Nat. Acad. Sci. USA, 77, 3312-3316.
- Reddy, G.P.V. and Pardee, A.B. (1982) J. Biol. Chem. 257 , 12526-12531.
- Roisin, M.P., and Kepes, A. (1978) Biochem. Biophys. Acta. 526 , 418-428.
- Schaller, M.B.O., Nusslein, V., Huf, J., Herrman, R., and Bonhoeffer, F. (1972), 63 , 183-200.

- Scocca, J.S., Panny, S.R., and Bessman M.J. (1969) J. Biol. Chem. 244 , 3698-3706.
- Stanley, W.M., Salas, M., Wahba, A., and Ochoa, S. (1966) Proc. Nat. Acad. Sci., 58 , 290.
- Tissiers, A.. (1974) in Ribosomes (Nomura, M., Tissieres, A., and Lengyel, P., Eds.), p. 6, Cold Spring Harbor Laboratory.
- Tomich, P.K., C.S. Chiu, M.G. Wovcha, and G.R. Greenberg. (1974). J. Biol. Chem. 249 , 7613-7622.
- Warner, H.R., and Snustad, D.P. (1983) in Bacteriophage T4 (Mathews, C.K., Kutter, E.M., Mosig, G., and Berget, P.B., Eds.), p. 103-109, Am. Soc. for Microbiology, Washington D.C.
- Wiberg, J.S. and Karam, J.D. (1983) in Bacteriophage T4 (Mathews, C.K., Kutter, E.M., Mosig, G. and Berget, P.B., Eds.), p. 193-201, Am. Soc. for Microbiology, Washington D.C.
- Wickremasinghe, R.G., Yaxley, J.C. and Hoffbrand, A.V. (1982) Eur. J. Biochem. 126 , 589-596.
- Williams, W.E. and Drake, J.W. (1977) Genetics 86 , 501-511.
- Wovcha, M.G., Chiu, C-S., Tomich, P.K. and Greenberg, G. R. (1976) J. Virol. 20 , 142-156.